

UNCLASSIFIED
~~CONFIDENTIAL~~

Copy 5
RM H58A03a

NACA RM H58A03a

c 2



RESEARCH MEMORANDUM

FLIGHT EVALUATION OF THE EFFECTS OF LEADING-EDGE-SLAT
SPAN ON THE STABILITY AND CONTROL CHARACTERISTICS
OF A SWEEP-WING FIGHTER-TYPE AIRPLANE DURING
ACCELERATED LONGITUDINAL MANEUVERS
AT TRANSONIC SPEEDS

By Gene J. Matranga and Katharine H. Armistead
High-Speed Flight Station
Edwards, Calif.

LIBRARY COPY
MAR 6 1958

CLASSIFIED DOCUMENT

This material contains information affecting the National Defense of the United States within the meaning of the espionage laws, Title 18, U.S.C., Secs. 793 and 794, the transmission or revelation of which in any manner to an unauthorized person is prohibited by law.
LANGLEY AERONAUTICAL LABORATORY
LIBRARY, NACA
LANGLEY FIELD, VIRGINIA

NATIONAL ADVISORY COMMITTEE FOR AERONAUTICS

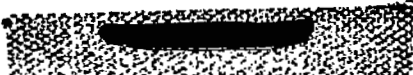
WASHINGTON
March 6, 1958

CLASSIFICATION CHANGED

To UNCLASSIFIED

By authority of TPA #14 effective Date 8-8-69

~~CONFIDENTIAL~~
UNCLASSIFIED


NATIONAL ADVISORY COMMITTEE FOR AERONAUTICS

RESEARCH MEMORANDUM

FLIGHT EVALUATION OF THE EFFECTS OF LEADING-EDGE-SLAT
SPAN ON THE STABILITY AND CONTROL CHARACTERISTICS
OF A SWEEP-WING FIGHTER-TYPE AIRPLANE DURING
ACCELERATED LONGITUDINAL MANEUVERS
AT TRANSONIC SPEEDS

By Gene J. Matranga and Katharine H. Armistead

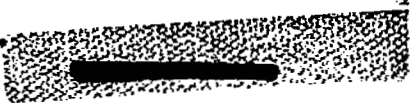
SUMMARY

A flight investigation consisting of accelerated longitudinal maneuvers was performed on a swept-wing fighter-type airplane utilizing several slat-span configurations to determine the effects of slat span on the stability and control characteristics of the airplane. The investigation was conducted essentially at an altitude of 40,000 feet.

For subsonic maneuvers as lift is increased to moderate values, a decrease in longitudinal stability, which manifests itself as a mild pitch-up in most instances, is evident in all configurations tested. Although reducing slat span improved these pitch-up characteristics in several instances, it always aggravated the lateral handling qualities and in several instances induced objectionable oscillations. At supersonic speeds no reduction of longitudinal stability due to change in lift is apparent.

The longitudinal stability and control characteristics generally are linear at low lift, and slat configuration has no appreciable effect on these characteristics.

Some measure of agreement is shown between the longitudinal stability data from flight and from wind tunnels at the lower angles of attack tested.



INTRODUCTION

A control problem of considerable severity has been encountered in recent years, especially with swept-wing airplanes, because of the rapid deterioration of longitudinal stability as angle of attack is increased at any given Mach number. In an attempt to alleviate this problem numerous wing devices have been employed, including the leading-edge slat. To investigate the effects of slat span on stability and control characteristics, and also to aid in the interpretation of wind-tunnel data obtained on models of a similar configuration (refs. 1 to 3), the NACA High-Speed Flight Station at Edwards, Calif., conducted tests on a swept-wing fighter-type airplane which incorporated free-floating leading-edge slats.

This paper presents the longitudinal stability and control characteristics for the test airplane over the speed range at a pressure altitude of 40,000 feet with all slats free-to-float, and for several slat-span configurations at Mach numbers of approximately 0.87, 0.95, and 1.13. Also discussed are the effects on the lateral handling qualities of the various slat configurations tested.

SYMBOLS

a_n	normal acceleration, g units
a_t	transverse acceleration, g units
b	wing span, ft
c	wing chord, ft
\bar{c}	mean aerodynamic chord, ft
C_N	airplane normal-force coefficient, $\frac{W a_n}{\frac{1}{2} \rho V^2 S}$
C_m	airplane pitching-moment coefficient, $\frac{\text{Pitching moment}}{\frac{1}{2} \rho V^2 S \bar{c}}$
$C_{m_{1t}}$	stabilizer effectiveness parameter, deg ⁻¹
$C_{m_q} + C_{m_{\dot{\alpha}}}$	longitudinal damping parameter, radians ⁻¹

$\frac{dC_m}{d\alpha}$	rate of change of airplane pitching-moment coefficient with angle of attack, deg^{-1}
$\frac{dC_m}{dC_N}$	rate of change of airplane pitching-moment coefficient with airplane normal-force coefficient
$\frac{dC_N}{d\alpha}$	rate of change of normal-force coefficient with angle of attack, deg^{-1}
$\frac{dF_{i_t}}{da_n}$	rate of change of stabilizer stick force with normal acceleration, lb/g
$\frac{di_t}{d\alpha}$	rate of change of stabilizer deflection with angle of attack
$\frac{di_t}{dC_N}$	rate of change of stabilizer deflection with airplane normal-force coefficient, deg
F_{i_t}	stabilizer stick force, lb
g	acceleration due to gravity, ft/sec^2
h_p	pressure altitude, ft
I_x	moment of inertia about X-axis, slug-ft^2
I_y	moment of inertia about Y-axis, slug-ft^2
I_z	moment of inertia about Z-axis, slug-ft^2
i_t	stabilizer deflection, deg
i_t'	stabilizer deflection, corrected to zero pitching acceleration, $i_t - \frac{I_y \dot{q}}{\frac{1}{2} \rho V^2 S \bar{c} C_{m_{i_t}}}, \text{deg}$
i_{t_0}	initial stabilizer setting, deg
M	Mach number

p	rolling velocity, radians/sec
\dot{p}	rolling acceleration, radians/sec ²
q	pitching velocity, radians/sec
\dot{q}	pitching acceleration, radians/sec ²
r	yawing velocity, radians/sec
\dot{r}	yawing acceleration, radians/sec ²
S	wing area, sq ft
t	time, sec
V	true velocity, ft/sec
W	airplane weight, lb
α	angle of attack, deg
β	angle of sideslip, deg
δ_a	total aileron deflection, deg
δ_r	rudder deflection, deg
δ_s	slat position, percent of full open position
δ_{st}	longitudinal control stick deflection, in.
ϵ	angle between body X-axis and principal X-axis, positive when body axis is above principal axis at airplane nose, deg
ρ	mass density of air, slugs/cu ft

Subscripts:

L	left
R	right

INSTRUMENTATION

The following quantities pertinent to this investigation were recorded on NACA internal recording instruments synchronized by a common timer:

- Airspeed and altitude
- Normal and transverse acceleration
- Angle of attack and angle of sideslip
- Stabilizer, rudder, and aileron deflection
- Pitching, yawing, and rolling velocity
- Pitching, yawing, and rolling acceleration
- Stabilizer stick force
- Slat position

Airspeed, altitude, and angle of attack were sensed on the nose boom. The angle of attack was corrected for the effects of pitching velocity only. The airspeed system was calibrated by the NACA radar phototheodolite method and is considered accurate to $M = \pm 0.02$ at transonic speeds and $M = \pm 0.01$ at supersonic speeds. The turnmeters used to measure the angular velocities and accelerations were referenced to the body axis of the airplane. The weight of the airplane was obtained from the pilot's report of the fuel remaining before each maneuver.

AIRPLANE

The airplane used in this investigation was a fighter type with low, swept, horizontal tail, and low, swept wings which incorporated midsemi-span ailerons and free-floating leading-edge slats. A single turbojet engine with afterburner powered the airplane. During the investigation, the airplane was flown with all slat segments free-floating, with one inboard slat segment locked closed on each wing, with two inboard slat segments locked closed on each wing, and with all slat segments locked closed.

A three-view drawing and a photograph of the airplane are shown in figures 1 and 2, respectively.

The physical characteristics of the airplane are presented in table I. Figure 3 shows the variation of the moments of inertia about the body axis and the inclination of the principal axis relative to the body axis based on the manufacturer's estimates for weight conditions expected in the normal flight range.

All control surfaces are irreversible, with spring bungees providing the pilot with forces proportional to the amount of surface deflection used. In addition, the longitudinal control system incorporates balance weights mounted just behind the control stick torque shaft. Figure 4, obtained from reference 4, presents the longitudinal stick force and stick deflection as a function of stabilizer position, exemplifying the nonlinear arrangement of the system.

TESTS

To evaluate the longitudinal stability and control characteristics of the airplane with all slats free-to-float, wind-up turns were performed over the speed range at an altitude of 40,000 feet.

The effects of slat span were to be determined by successively locking slat segments closed and performing wind-up turns. The initial condition tested was the configuration with the inboard slat segment on each wing locked closed. It was planned to lock additional segments closed until the condition with all slats locked closed would be reached. However, with the two inboard slat segments locked closed severe oscillatory motions were encountered with increase of angle of attack in the wind-up turns. Therefore, the only other configuration tested was with all slats locked closed. All maneuvers were performed essentially at an altitude of 40,000 feet and at Mach numbers of 0.87, 0.95, and 1.13.

The center-of-gravity position remained about 30 percent of the mean aerodynamic chord throughout all tests.

All maneuvers in this investigation were initiated from near 1g conditions. The angle-of-attack and normal-force-coefficient variations with Mach number for 1g flight at 40,000 feet at a nominal weight of 22,000 pounds are presented in figure 5.

RESULTS AND DISCUSSION

General

Representative time histories of wind-up turns with all slats free-to-float and all slats locked closed for Mach numbers of about 0.87, 0.95, and 1.13 at an altitude of 40,000 feet are presented in figures 6 and 7, respectively. Stability and control plots for the configurations with all slats free-floating, one slat locked closed, two slats locked closed, and all slats locked closed are presented in figures 8 to 11, respectively.

The values of the pitching-moment coefficient presented in figures 8 to 11 were obtained from the following equation:

$$C_m = \frac{I_y}{\frac{1}{2}\rho V^2 S \bar{c}} \dot{q} - \left[C_{m_{i_t}} (i_t - i_{t0}) \right] - \frac{\bar{c}}{2V} (C_{m_q} + C_{m_{\dot{\alpha}}}) q$$

Figure 12 presents the stabilizer effectiveness parameter from unpublished data and the longitudinal damping parameter from reference 5, both obtained from stabilizer pulse maneuvers. These parameters, used to calculate the flight-obtained pitching-moment curves, were assumed to be valid for all configurations tested and over the lift ranges tested.

As angle of attack is increased to moderate values, the data below $M = 1.0$ show a decrease in longitudinal stability for all configurations tested. The supersonic data normally exhibit no deviation from linearity due to the change of angle of attack and lift.

Because of the arrangement of the nonlinear longitudinal control gearing, as shown in figure 4, the stick-force gradient dF_{i_t}/da_n produces an apparent reduction of stability at elevated g under all conditions tested, and in some instances a stick-free instability exists.

The stability and control characteristics which are presented in figure 13 were taken in the low-lift, low angle-of-attack region under all conditions tested. These data exhibit the typical transonic-supersonic trends expected of a swept-wing airplane. No appreciable differences in these data are found when comparing the various configurations tested.

Effect of Slat Configuration on Handling Qualities

A comparison of the variation of the pitching-moment curve with angle of attack for the four configurations tested at typical Mach numbers is presented in figure 14. At all subsonic speeds a reduction in stability, which in most instances was reported by the pilot to manifest itself as a mild pitch-up, is indicated by the data. Above the region of reduced stability, an area of positive stability normally exists. An uncomfortable pitch-down did occur, however, when recovering from a pitch-up condition with slightly excessive control input reinforcing the natural tendency to pitch down. Although an increase in Mach number from 0.87 to 0.95 noticeably increases the static margin, the angle of attack for which the decrease of stability occurs is usually reduced. Rate-of-control input had no noticeable effect on the handling qualities of the airplane, according to the pilot.

At a Mach number of 0.87 the airplane with all slat segments free-to-float follows the general trends discussed. Locking the inboard slat closed on each wing, resulted in a milder pitch-up than with all slats free-floating, the pilot reported, but mild lateral oscillations were evident just prior to the pitch. This milder pitch-up was not borne out by the data presented in figure 14, however. In the opinion of the pilot, locking two slats closed resulted in heavy buffet and "wicked" longitudinal oscillations at moderate angles of attack. Sharp wing dropping at elevated lift considerably restricted maneuverability. With all slats locked closed, along with a mild pitch-up which is shown clearly in the data, objectionable lateral and longitudinal oscillations occurred.

Increasing Mach number to 0.95, introduced mild lateral oscillations to the normal trends noted with all slats free-to-float. Locking one slat closed resulted in mild-to-moderate lateral oscillations and definite wing dropping. When two slats were locked closed, the pilot reported no pitch-up, but he believed the pitch-up indicated by the data could have been masked by the severe wing dropping and oscillations experienced in this configuration. Figures 15 and 16 are time histories of the "wicked" oscillatory and wing-dropping motions found so objectionable by the pilot. With all slats locked closed, the lateral oscillations and wing dropping were again quite objectionable.

Although it is quite evident from figure 14 that reducing slat span slightly improved the pitching-moment characteristics of the airplane in several instances (notably the condition with two slat segments locked closed), objectionable longitudinal and lateral oscillations as well as severe wing dropping, such as presented in figures 15 and 16, prevented the pilot from appreciating these improvements in the pitching-moment characteristics.

The supersonic data show little or no change for the various configurations. Still, as noted previously, lateral sensitivity was more evident as additional slat segments were locked closed. No supersonic pitch-up was encountered in this investigation.

In unaccelerated stalls as slat span was decreased, lateral motions became more pronounced, as in the turns, and the onset of buffet occurred at higher speeds. However, no particularly adverse characteristics were noted.

Comparison of Flight and Wind-Tunnel Data

As noted in the INTRODUCTION, several wind-tunnel investigations were performed to determine the longitudinal stability of models having a configuration similar to the test swept-wing fighter-type airplane.

These wind-tunnel data served as a guide for the flight investigation. A comparison of the flight data with the wind-tunnel data from reference 3 at a Mach number of 0.95 is shown in figure 17. The wind-tunnel data were corrected to the flight test center-of-gravity position.

Considering all the variables which enter into this comparison, agreement is reasonably good at lower angles of attack. Differences at the higher angles of attack could easily arise from the fact that in calculating the pitching moments from flight data, constant values for $C_{m_{i,t}}$ and $C_{m_q} + C_{m_{\dot{\alpha}}}$ were assumed over the lift range. The Mach number chosen is in the region where slight variations of speed can have considerable effect. Also, there are several physical differences between the model and the test airplane. Among these differences are the degree of slat rotation (the model slats rotated 10° , whereas the airplane slats rotate 15°), the slat operation (the model slats were locked open or closed, whereas the airplane slats are free-floating), and the wing plan form (the model wing is similar to the original prototype airplane to which 12-inch wing-span tip extensions subsequently have been added on the airplane, changing the wing area, span, aspect ratio, and taper ratio).

This investigation has emphasized that, although wind-tunnel investigations can provide data with which the longitudinal handling qualities may be computed, a dynamic analysis is necessary to determine the overall longitudinal handling qualities required for flight guidance. Furthermore, flight studies are required to determine lateral handling qualities which might tend to mask the longitudinal characteristics.

CONCLUSIONS

From the results of flight tests of several slat-span configurations on a swept-wing fighter-type airplane incorporating segmented free-floating slats at an altitude of 40,000 feet it may be concluded that:

1. For subsonic maneuvers as lift is increased to moderate values, a decrease in longitudinal stability, which manifests itself as a mild pitch-up in most instances, is evident in all configurations tested. Reducing slat span improved these pitch-up characteristics in several instances, but it also aggravated the lateral handling qualities and in some instances induced objectionable oscillations. At supersonic speeds no reductions of longitudinal stability due to change in lift is apparent.

2. The longitudinal stability and control characteristics generally are linear at low lift, and slat configuration has no appreciable effect on these characteristics.

3. For all slat configurations, some measure of agreement is shown between the longitudinal stability data from flight and wind-tunnel tests at the lower angles of attack tested. The poor agreement between flight and wind-tunnel data at the higher angles of attack is attributed to the geometric differences between the wind-tunnel model and the airplane, and the fact that constant values of derivatives were used to calculate the pitching-moment curves at all lifts.

High-Speed Flight Station,
National Advisory Committee for Aeronautics,
Edwards, Calif., December 12, 1957.

REFERENCES

1. Runckel, Jack F., and Steinberg, Seymour: Effects of Leading-Edge Slats on the Aerodynamic Characteristics of a 45° Sweptback Wing-Fuselage Configuration at Mach Numbers of 0.4 to 1.03. NACA RM L53F23, 1953.
2. Arabian, Donald D., Runckel, Jack F., and Reid, Charles F., Jr.: Aerodynamic Load Measurements and Opening Characteristics of Automatic Leading-Edge Slats on a 45° Sweptback Wing at Transonic Speeds. NACA RM L53I30, 1954.
3. Runckel, Jack F., and Schmeer, James W.: The Aerodynamic Characteristics at Transonic Speeds of a Model With a 45° Sweptback Wing, Including the Effect of Leading-Edge Slats and a Low Horizontal Tail. NACA RM L53J08, 1954.
4. Surface Controls Group, N.A.A.: Calculated Data for Primary Control Systems of the YF-100A, F-100A, and F-100C Airplanes. Rep. No. NA-52-376-2, North American Aviation, Inc., July, 1955.
5. Wolowicz, Chester H.: Dynamic Longitudinal Stability Characteristics of a Swept-Wing Fighter-Type Airplane at Mach Numbers Between 0.36 and 1.45. NACA RM H56H03, 1957.

TABLE I.- PHYSICAL CHARACTERISTICS OF THE AIRPLANE

Wing:	
Airfoil section	NACA 64A007
Total area (including aileron and 89.84 sq ft covered by fuselage), sq ft	385.21
Span, ft	58.98
Mean aerodynamic chord, ft	11.16
Root chord, ft	15.66
Tip chord, ft	4.15
Taper ratio	0.262
Aspect ratio	3.86
Sweep at 0.25 chord line, deg	45
Incidence, deg	0
Dihedral, deg	0
Geometric twist, deg	0
Aileron:	
Area rearward of hinge line (each), sq ft	19.32
Span at hinge line (each), ft	7.81
Chord rearward of hinge line, percent wing chord	25
Travel (each), deg	±15
Leading-edge slat:	
Span, equivalent, ft	12.71
Segments	5
Spanwise location, inboard end, percent wing semispan	25.5
Spanwise location, outboard end, percent wing semispan	89.2
Ratio of slat chord to wing chord (parallel to fuselage reference line), percent	20
Rotation, maximum, deg	15
Horizontal tail:	
Airfoil section	NACA 65A005.5
Total area (including 31.65 sq ft covered by fuselage), sq ft	98.86
Span, ft	18.72
Mean aerodynamic chord, ft	5.85
Root chord, ft	8.14
Tip chord, ft	2.46
Taper ratio	0.30
Aspect ratio	5.54
Sweep at 0.25 chord line, deg	45
Dihedral, deg	0
Travel, leading edge up, deg	5
Travel, leading edge down, deg	25
Control system	Irreversible hydraulic boost and artificial feel
Vertical tail:	
Airfoil section	NACA 65A005.5
Area (excluding dorsal fin and area blanketed by fuselage), sq ft	42.7
Area blanketed by fuselage (area between fuselage contour line and line parallel to fuselage reference line through intersections of leading edge of vertical tail and fuselage contour line), sq ft	2.45
Span (unblanketed), ft	7.93
Mean aerodynamic chord, ft	5.90
Root chord, ft	8.28
Tip chord, ft	2.49
Taper ratio	0.301
Aspect ratio	1.49
Sweep at 0.25 chord line, deg	45
Rudder:	
Area, rearward of hinge line, sq ft	6.3
Span at hinge line, ft	3.33
Root chord, ft	2.27
Tip chord, ft	1.50
Travel, deg	±20
Spanwise location, inboard end, percent vertical-tail span	5.1
Spanwise location, outboard end, percent vertical-tail span	44.8
Chord, percent vertical-tail chord	28.4
Balance	Aerodynamic
Fuselage:	
Length (afterburner nozzle closed), ft	45.64
Maximum width, ft	5.98
Maximum depth over canopy, ft	6.37
Side area (total), sq ft	230.92
Finesse ratio (afterburner nozzle closed)	7.86
Speed brake:	
Surface area, sq ft	14.14
Maximum deflection, deg	50
Powerplant:	
Turbojet engine	One Pratt & Whitney J57-P21 with afterburner
Thrust (guarantee sea level), afterburner, lb	16,000
Military, lb	10,000
Normal, lb	9,000
Airplane weight, lb:	
Basic (without fuel, oil, water, pilot)	20,262
Total (full fuel, oil, water, pilot)	25,400
Center-of-gravity location, percent \bar{c}:	
Total weight - gear down	30.2
Total weight - gear up	30.2

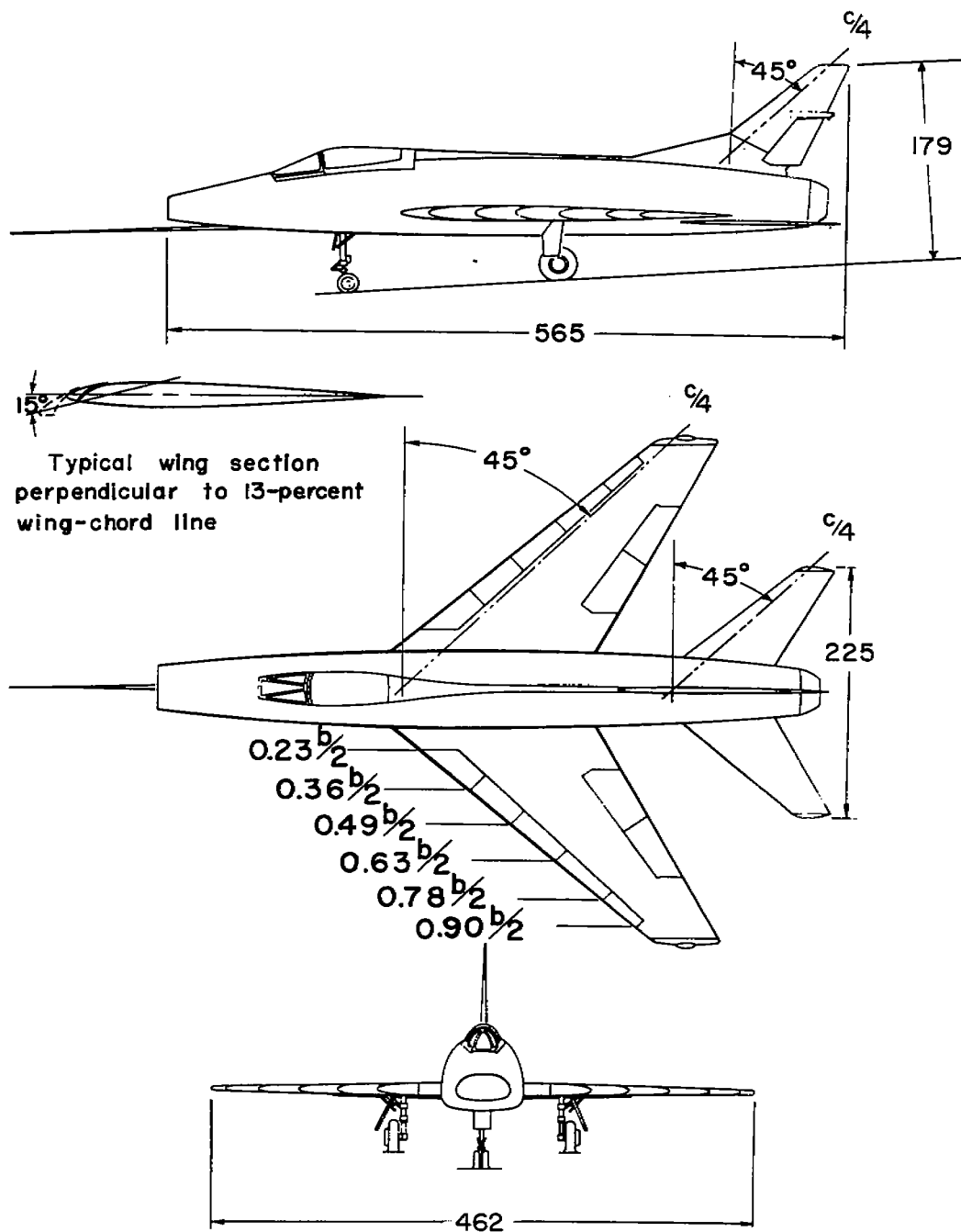
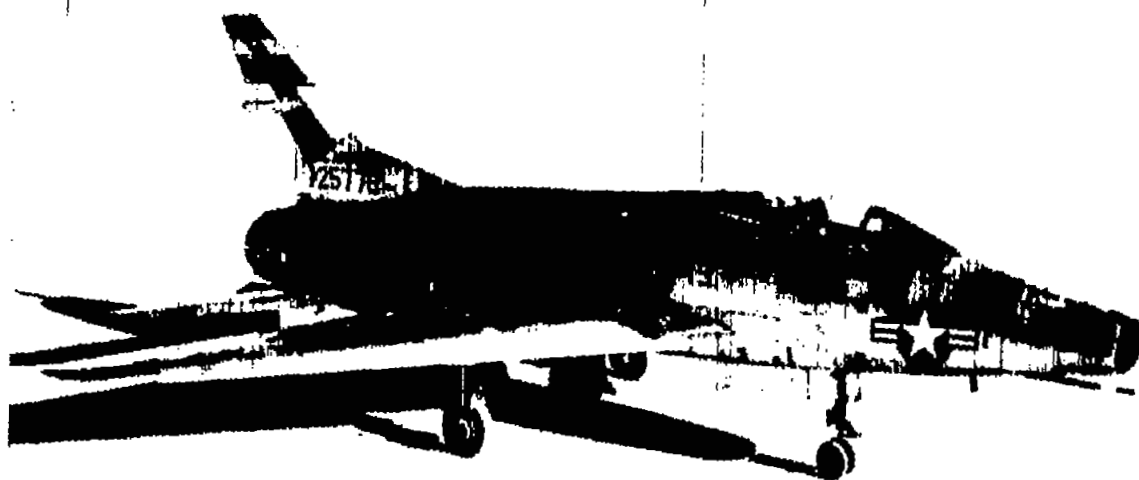


Figure 1.- Three-view drawing of the test airplane. All dimensions in inches.



E-2097
Figure 2.- Photograph of the airplane with the slats in the extended position.

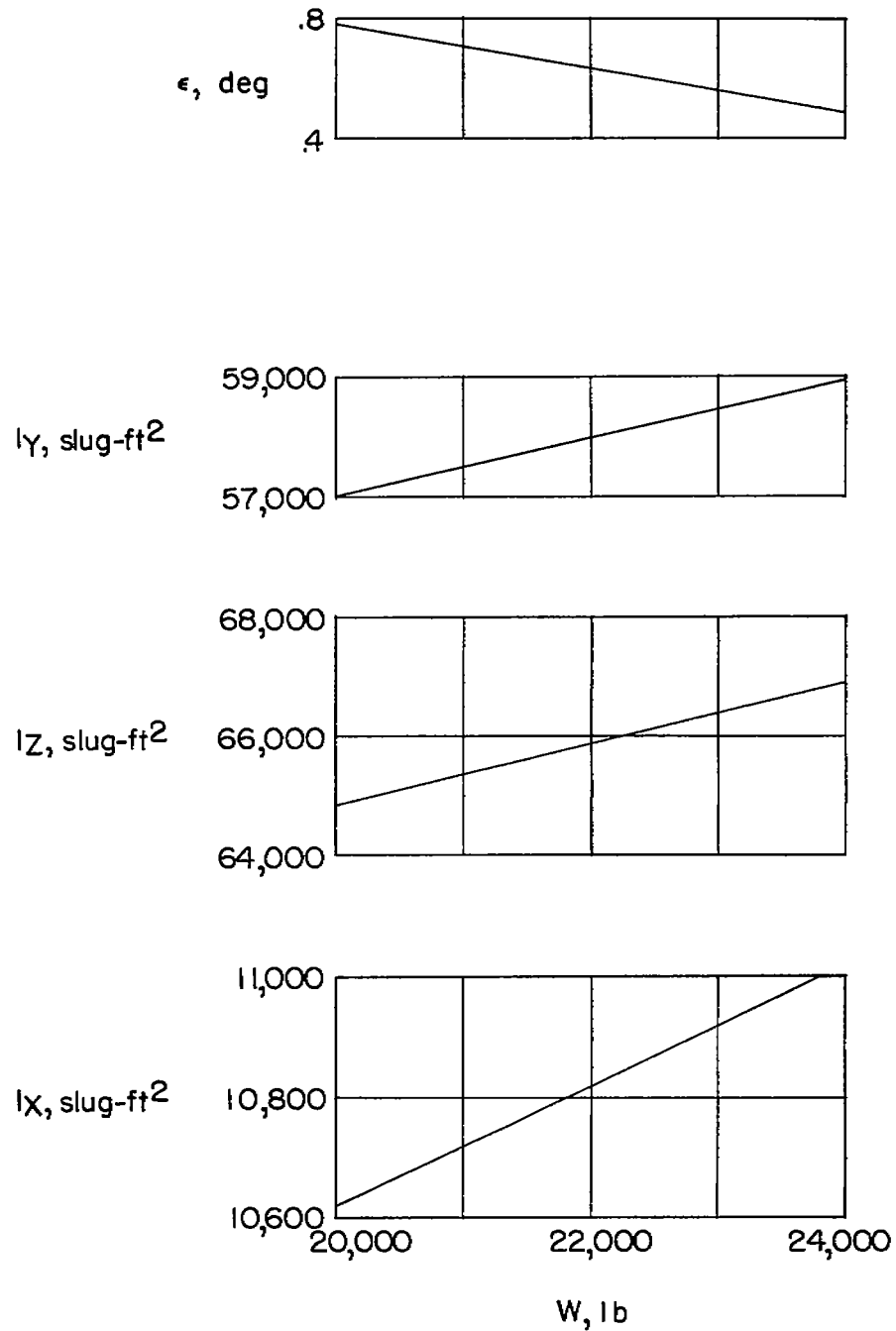


Figure 3.- Approximated variation of the principal moments of inertia and inclination of principal axis relation to the body axis.

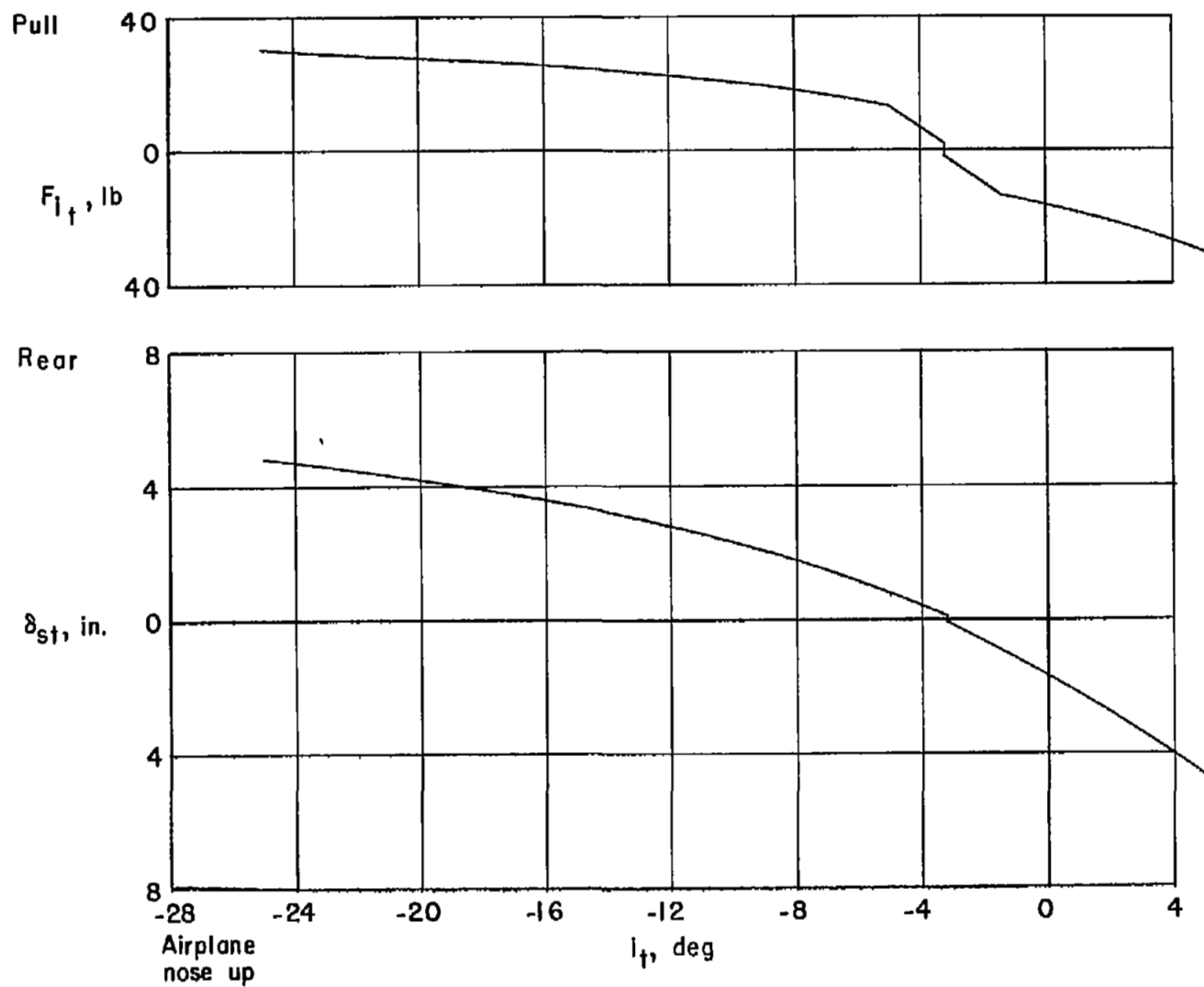


Figure 4.- Variation of longitudinal control force and stick deflection with stabilizer position.

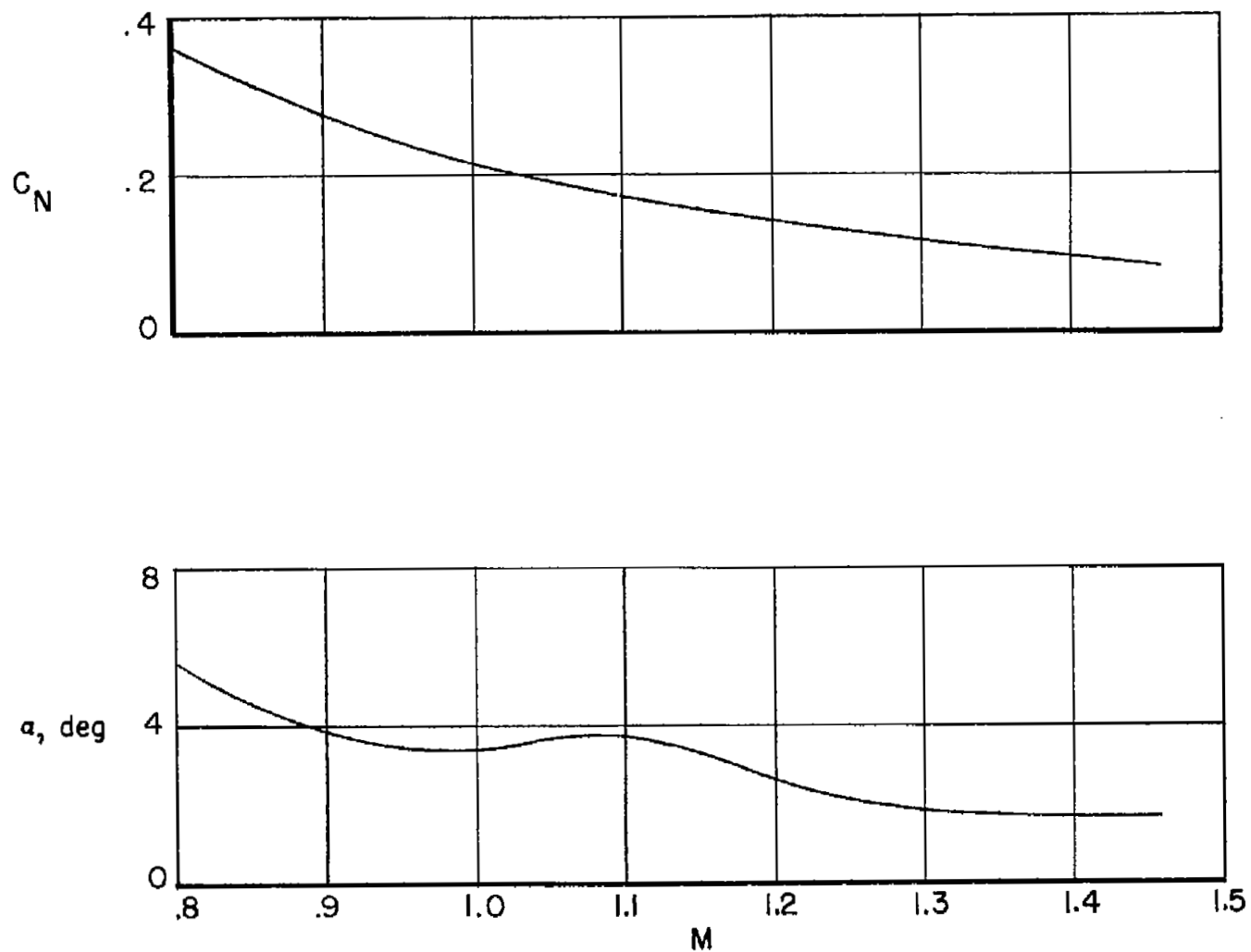


Figure 5.- Variation of trim normal-force coefficient and angle of attack with Mach number for 1g flight at 40,000 feet at a normal weight of 22,000 pounds. All slats free to float.

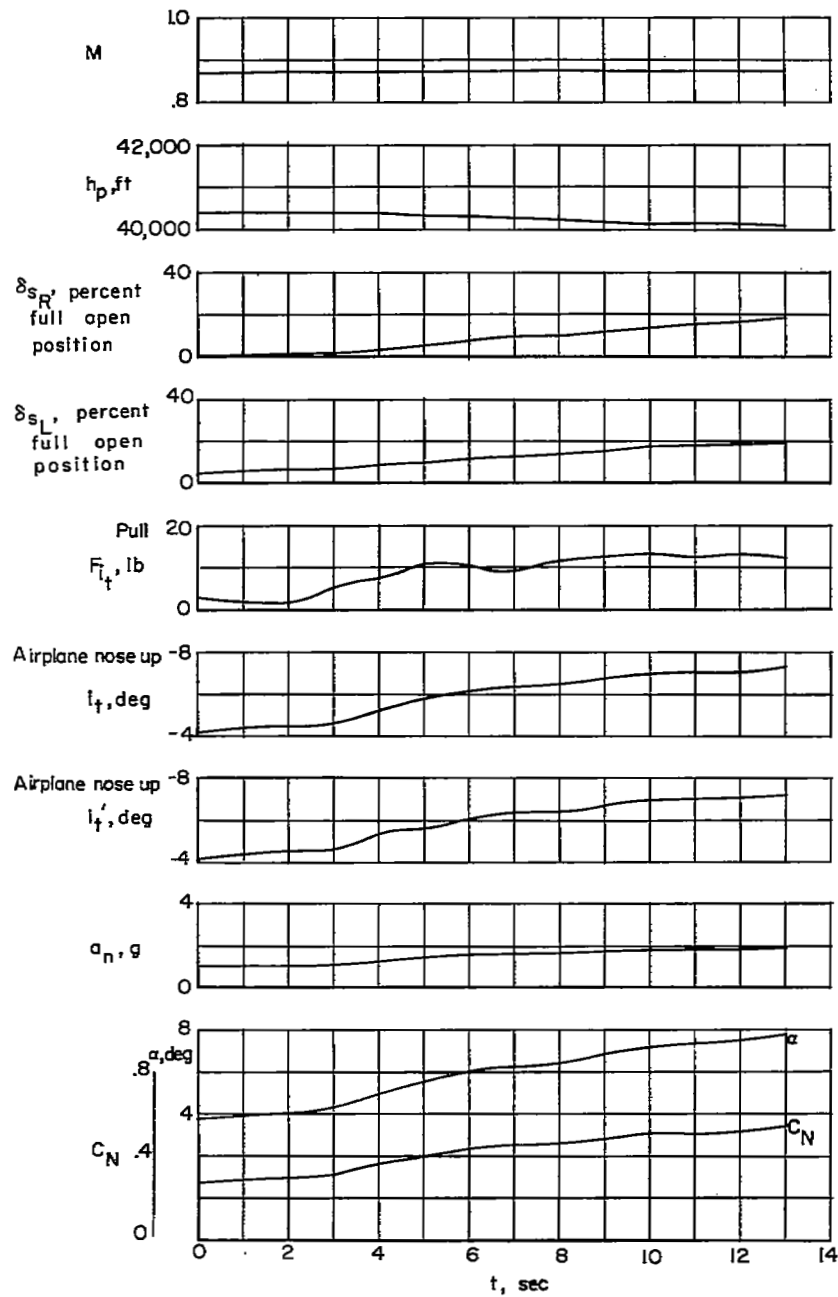
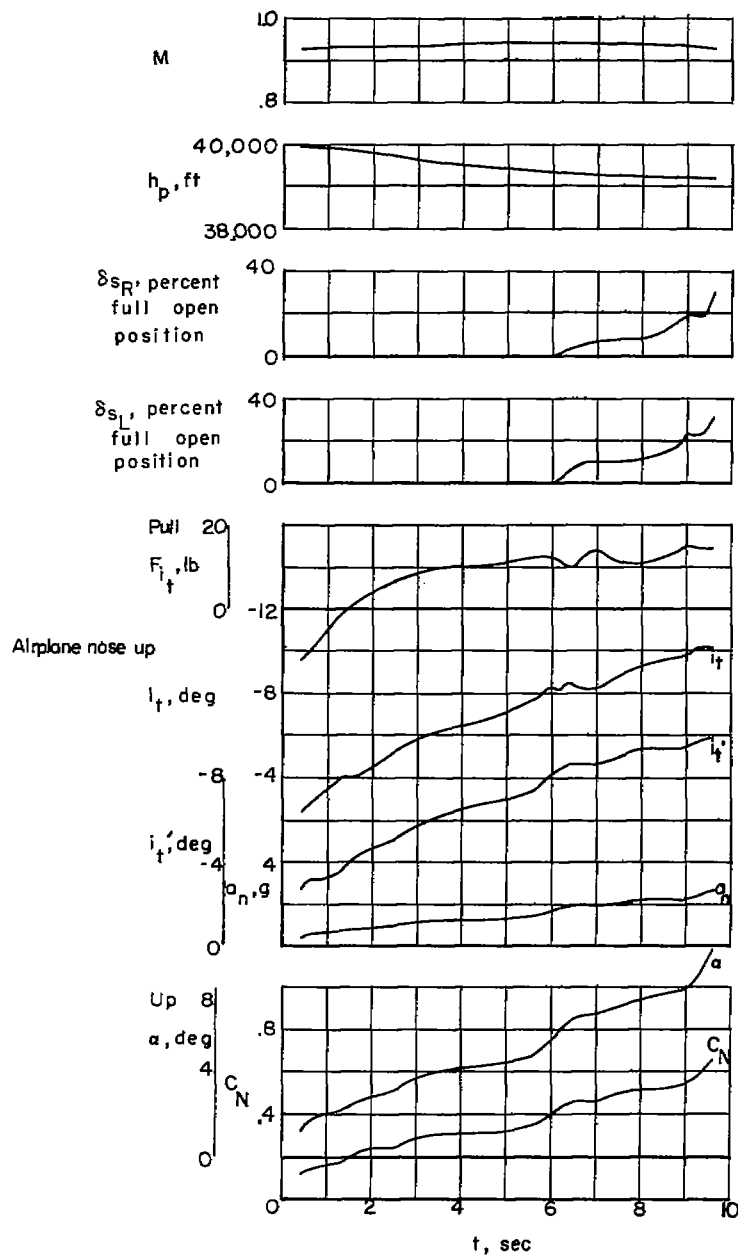
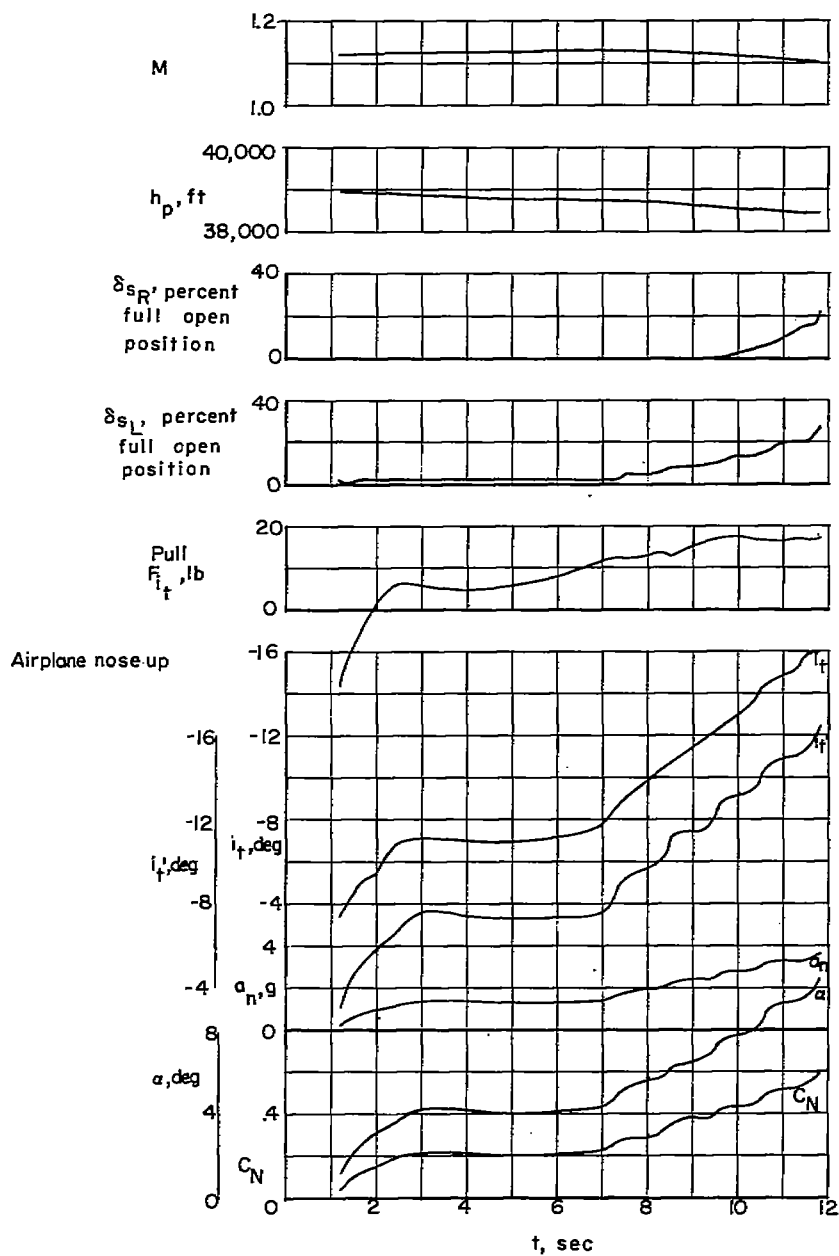
(a) $M \approx 0.875$; $h_p \approx 40,000$ ft.

Figure 6.- Time history of a wind-up turn. All slats free to float.



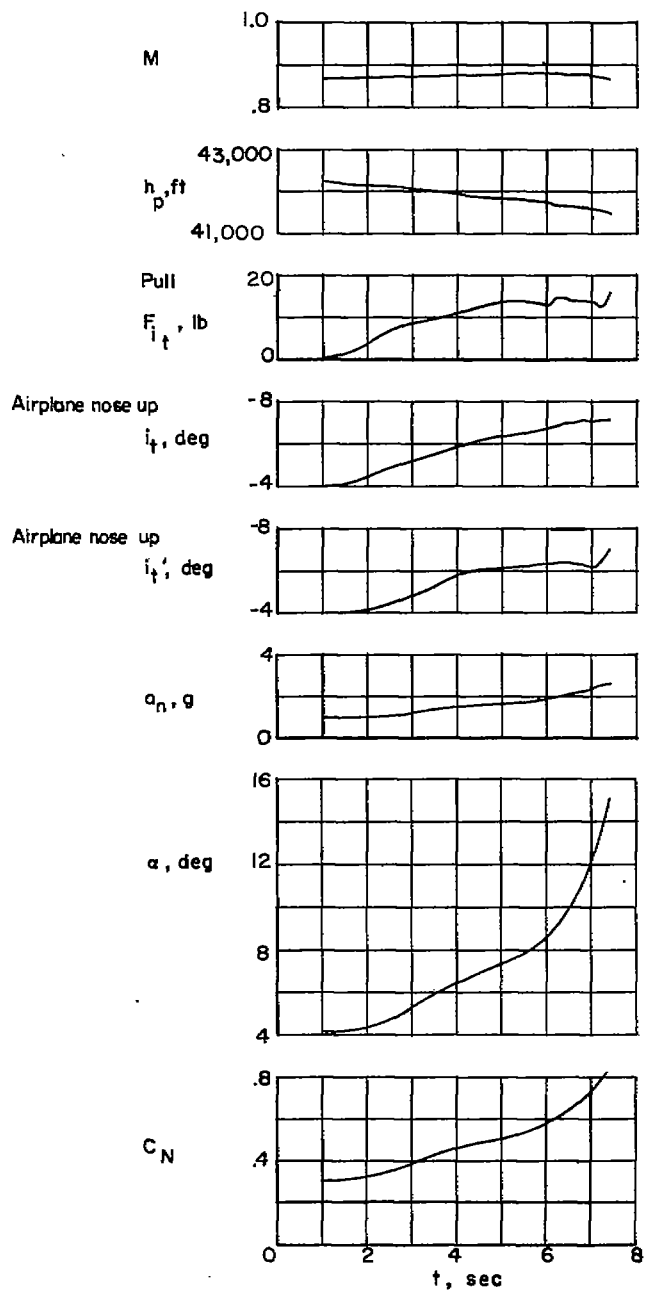
(b) $M \approx 0.935$; $h_p \approx 40,000$ ft.

Figure 6.- Continued.



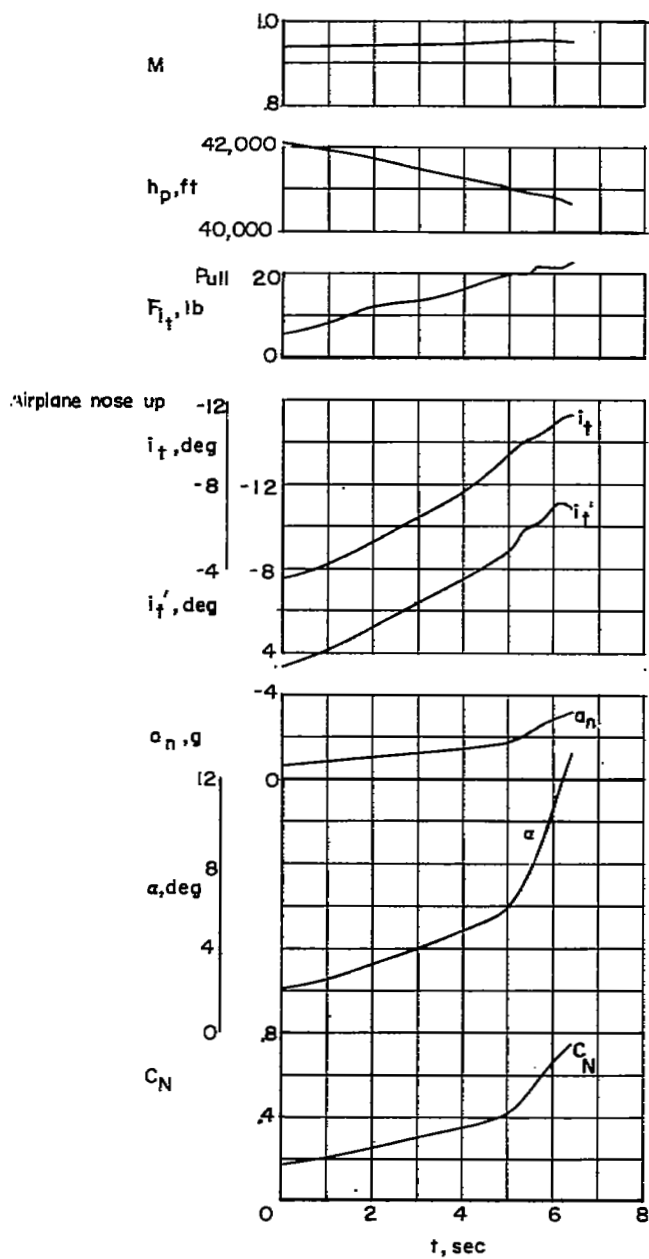
(c) $M \approx 1.125$; $h_p \approx 40,000$ ft.

Figure 6.- Concluded.



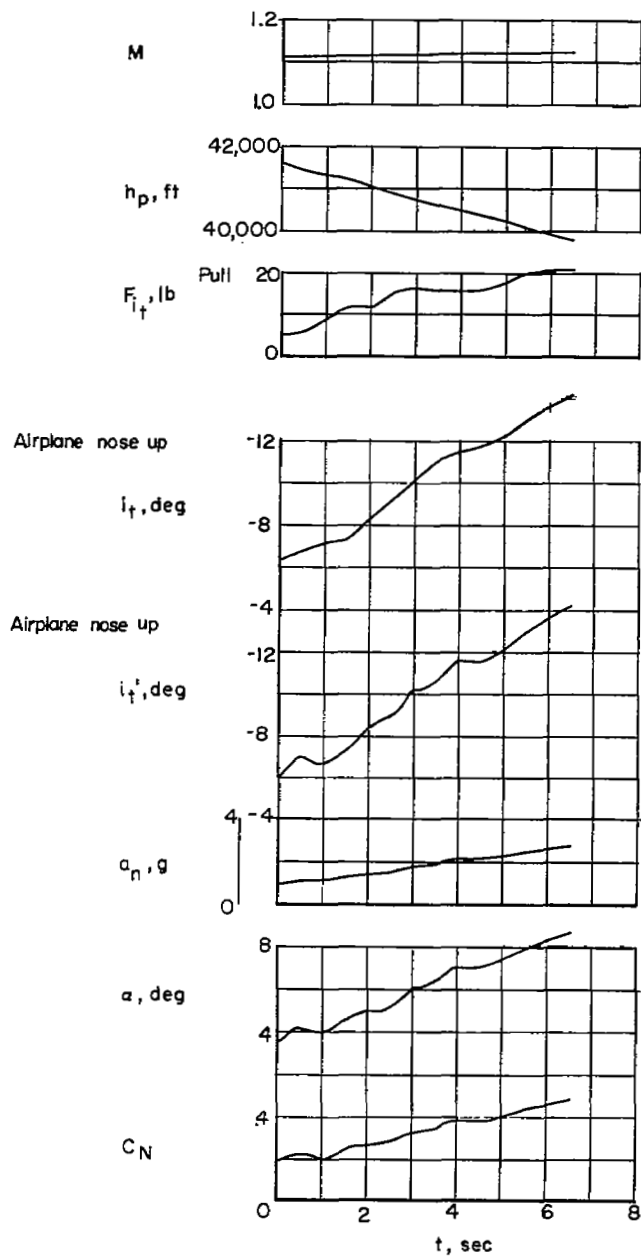
(a) $M \approx 0.875$; $h_p \approx 40,000$ ft.

Figure 7.- Time history of a wind-up turn. All slats locked closed.



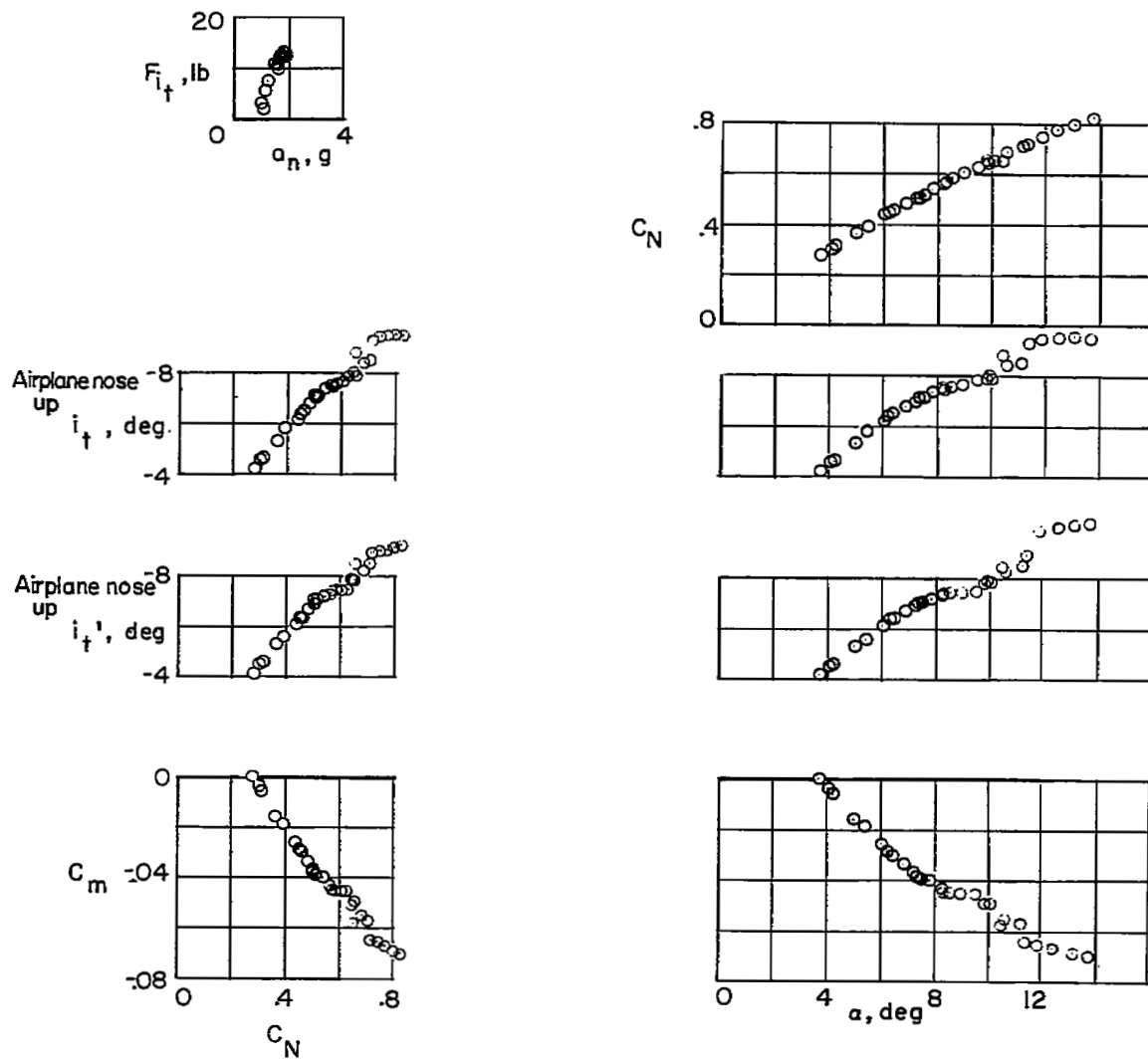
(b) $M \approx 0.950$; $h_p \approx 40,000$ ft.

Figure 7.- Continued.



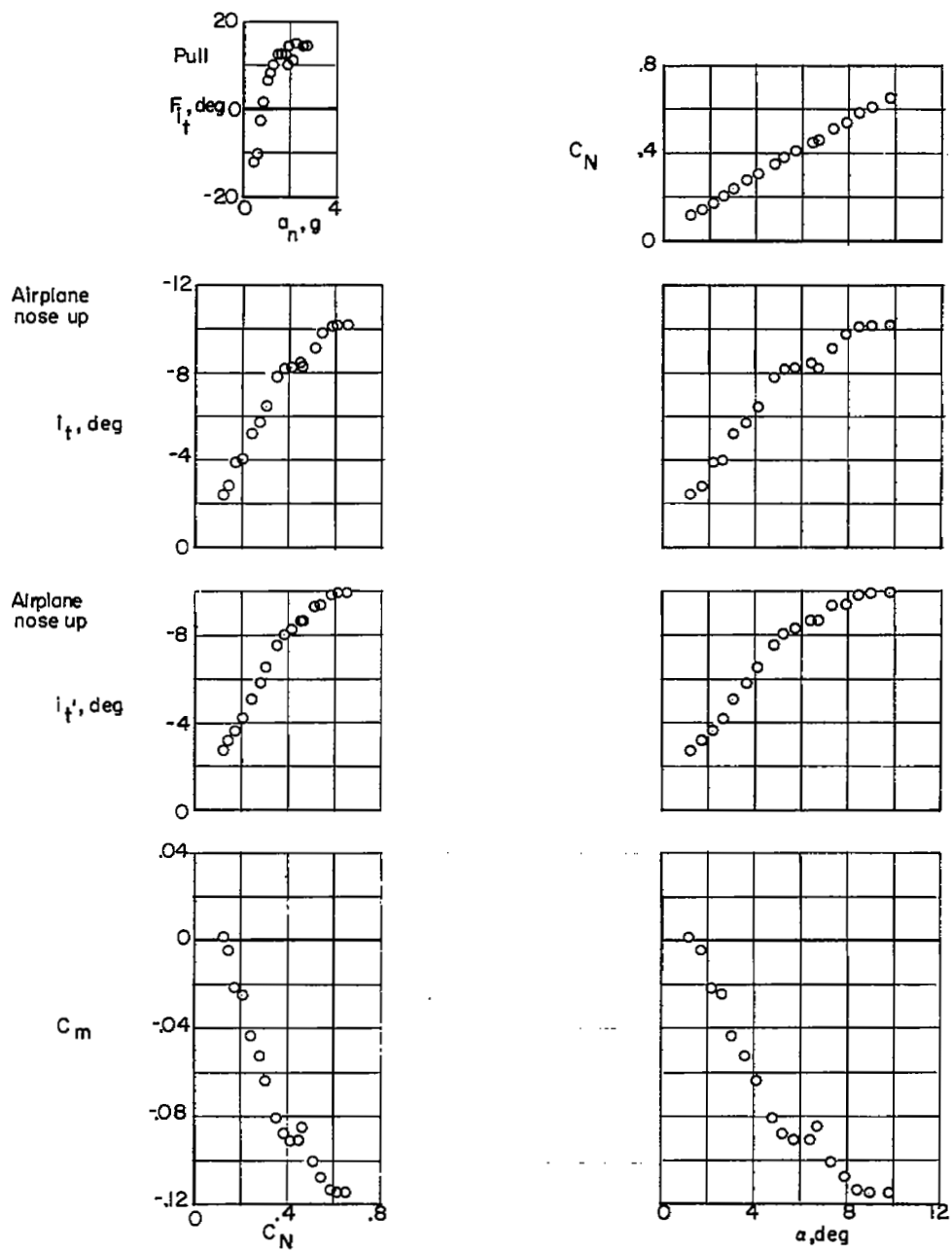
(c) $M \approx 1.115$; $h_p \approx 40,000$ ft.

Figure 7.- Concluded.



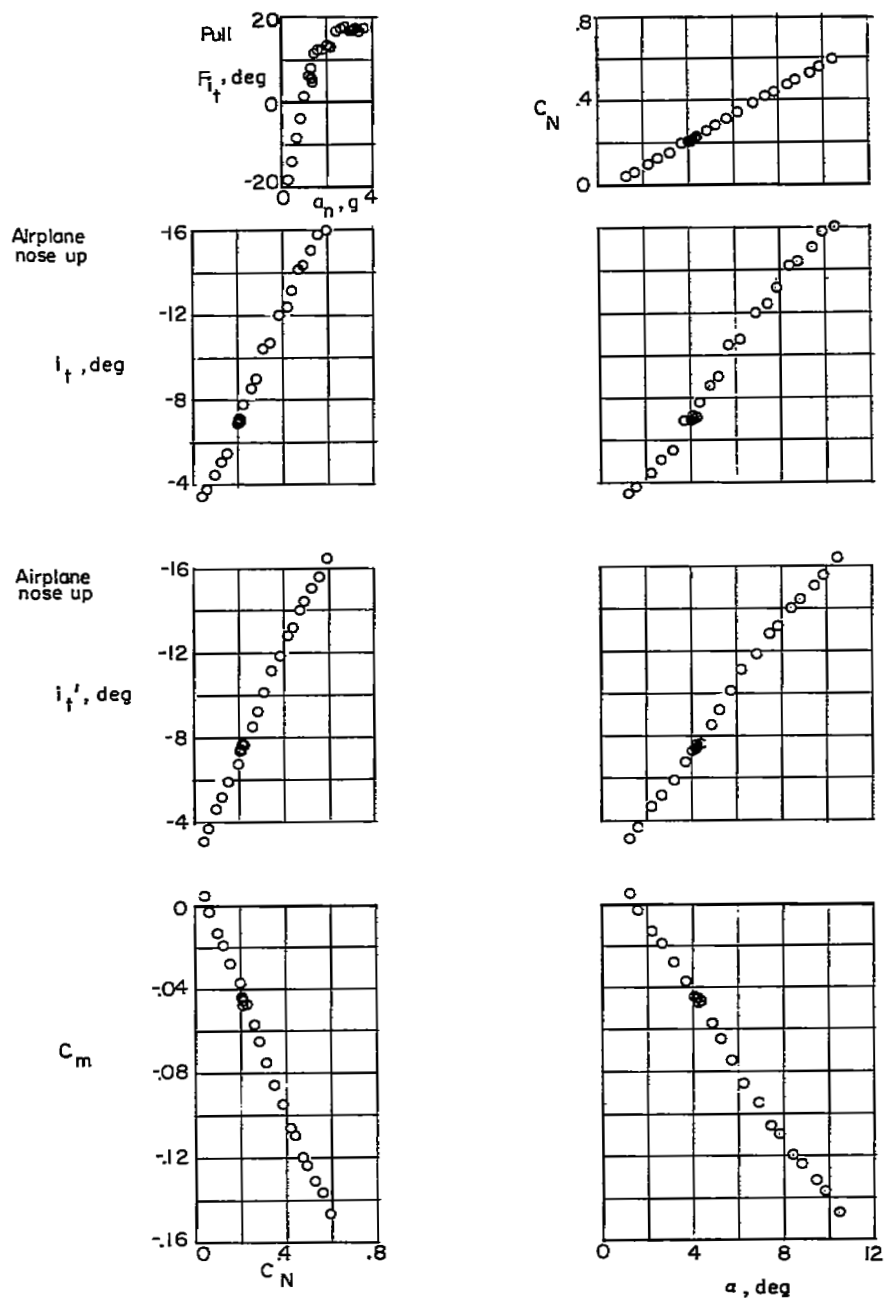
(a) $M \approx 0.875$; $h_p \approx 40,000$ ft.

Figure 8.- Variation of several stability and control characteristics during a wind-up turn. All slats free to float.



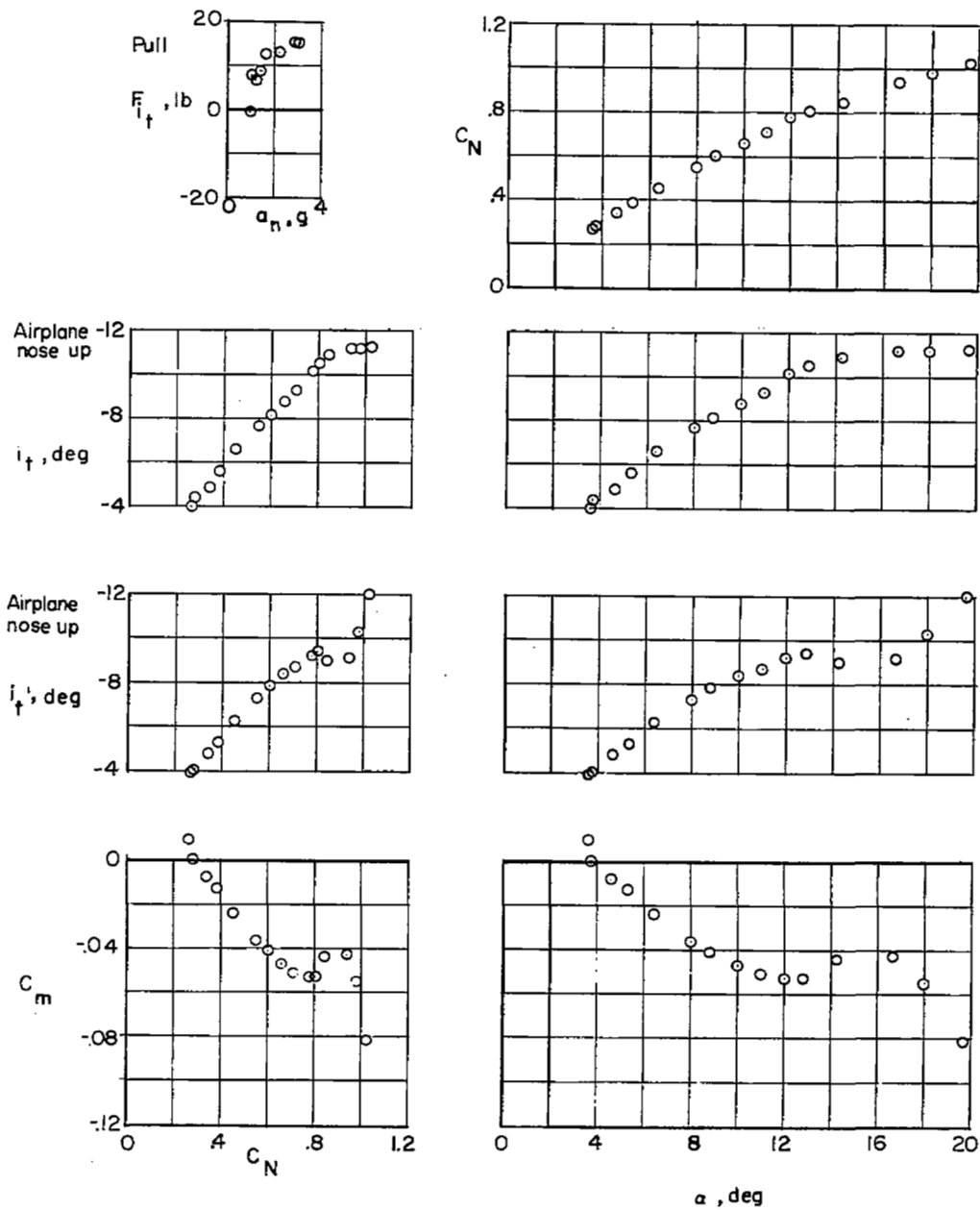
(b) $M \approx 0.935$; $h_p \approx 40,000$ ft.

Figure 8.- Continued.



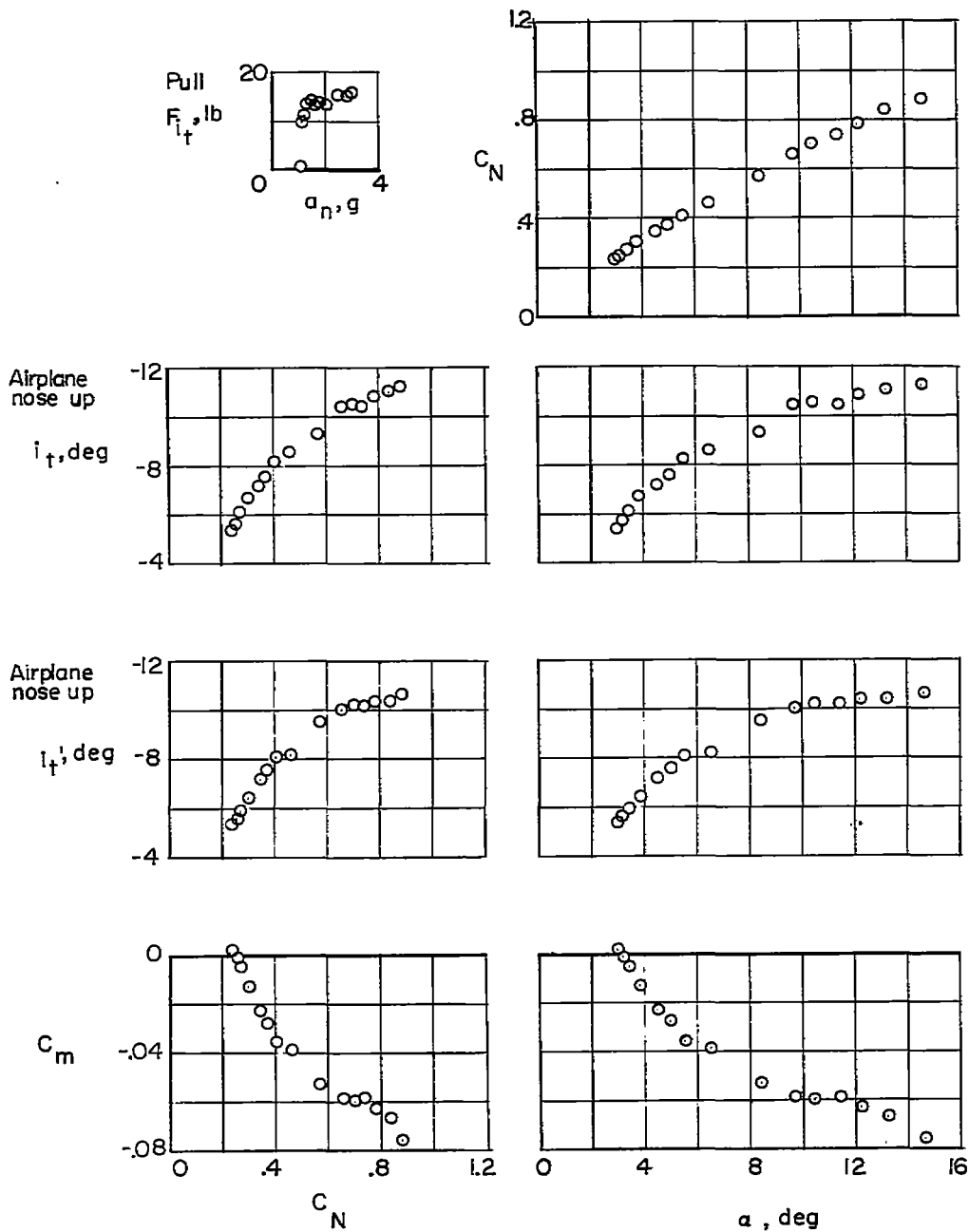
(c) $M \approx 1.125$; $h_p \approx 40,000$ ft.

Figure 8.- Concluded.



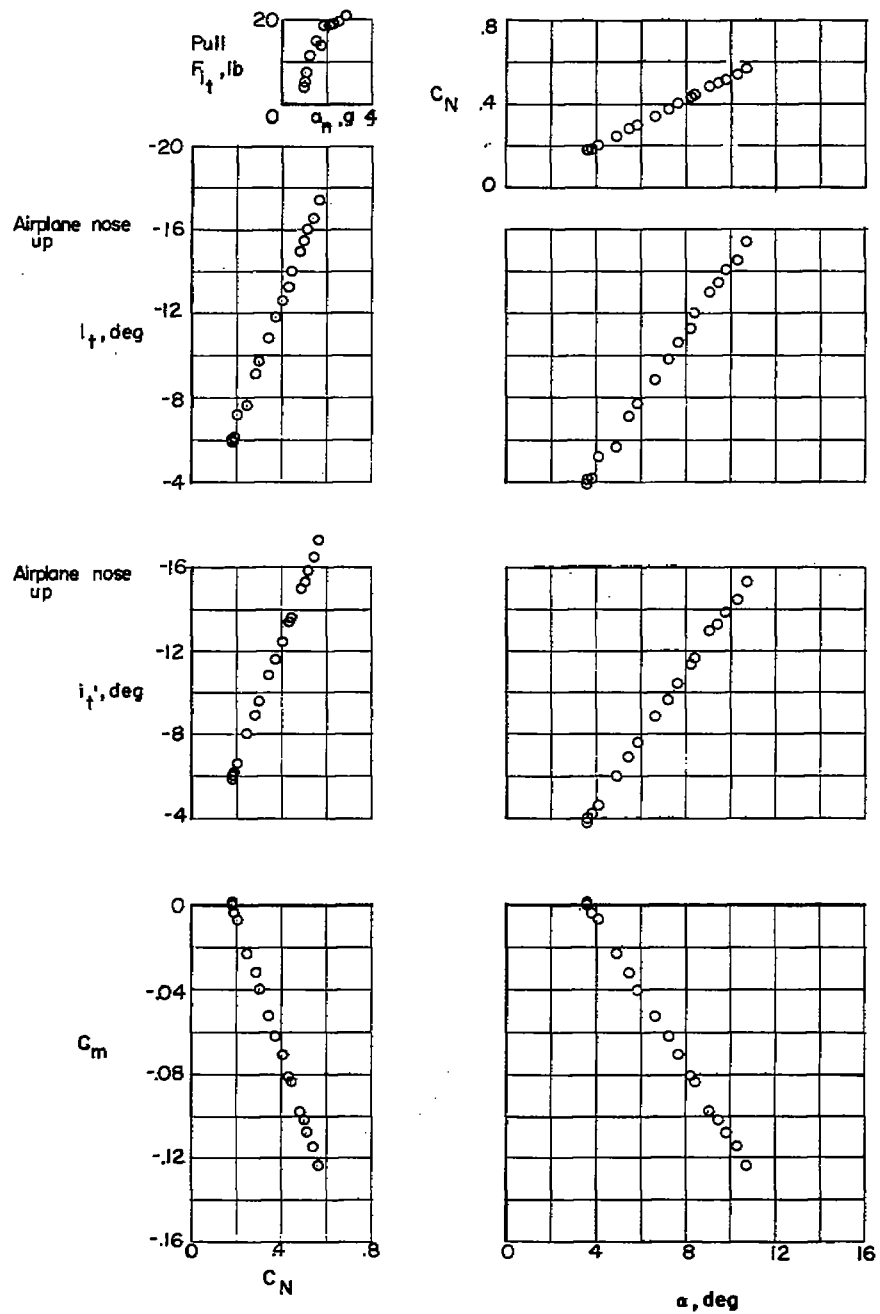
(a) $M \approx 0.875$; $h_p \approx 40,000$ ft.

Figure 9.- Variation of several stability and control characteristics during a wind-up turn. One inboard slat segment locked closed.



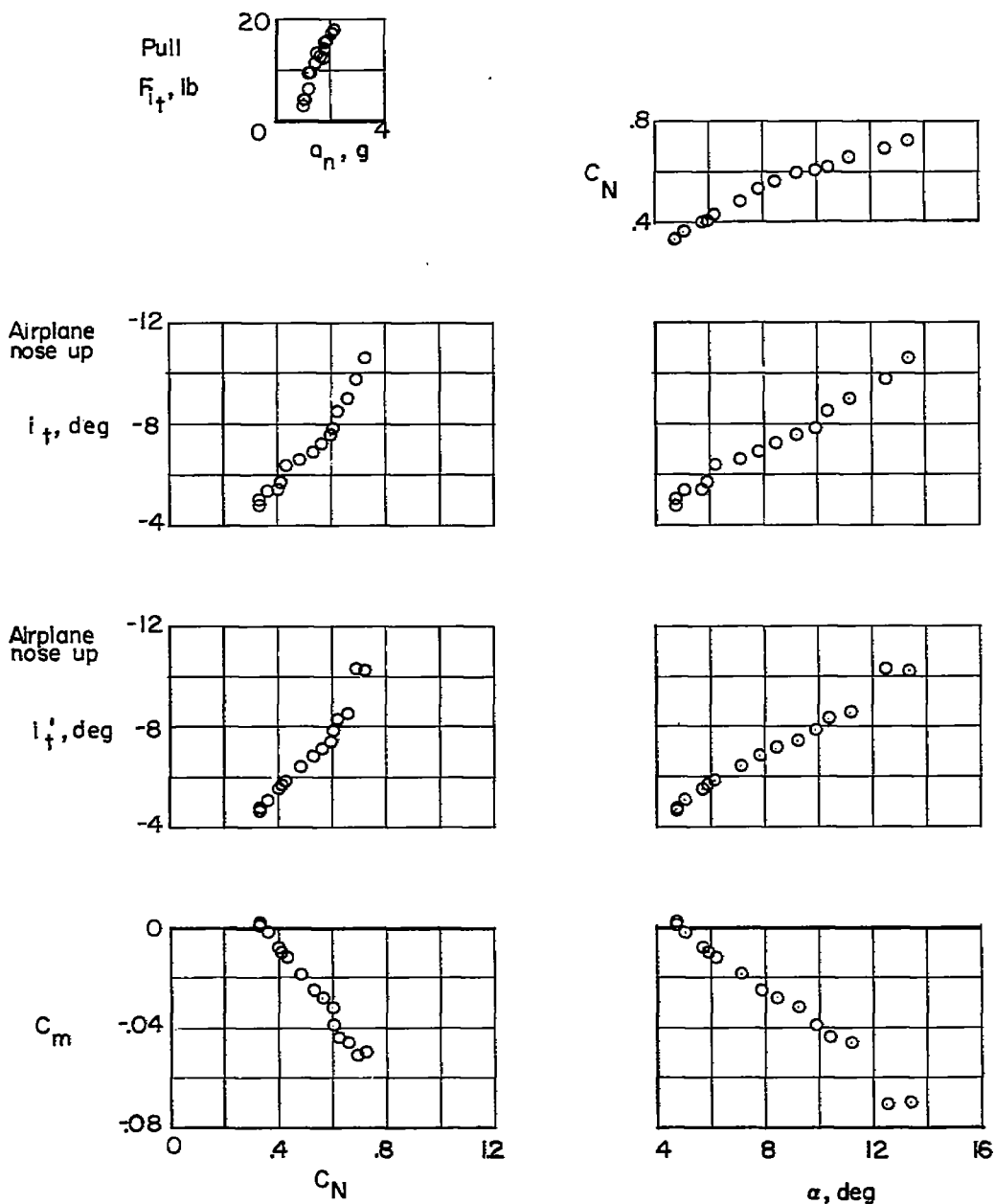
(b) $M \approx 0.945$; $h_p \approx 40,000$ ft.

Figure 9.- Continued.



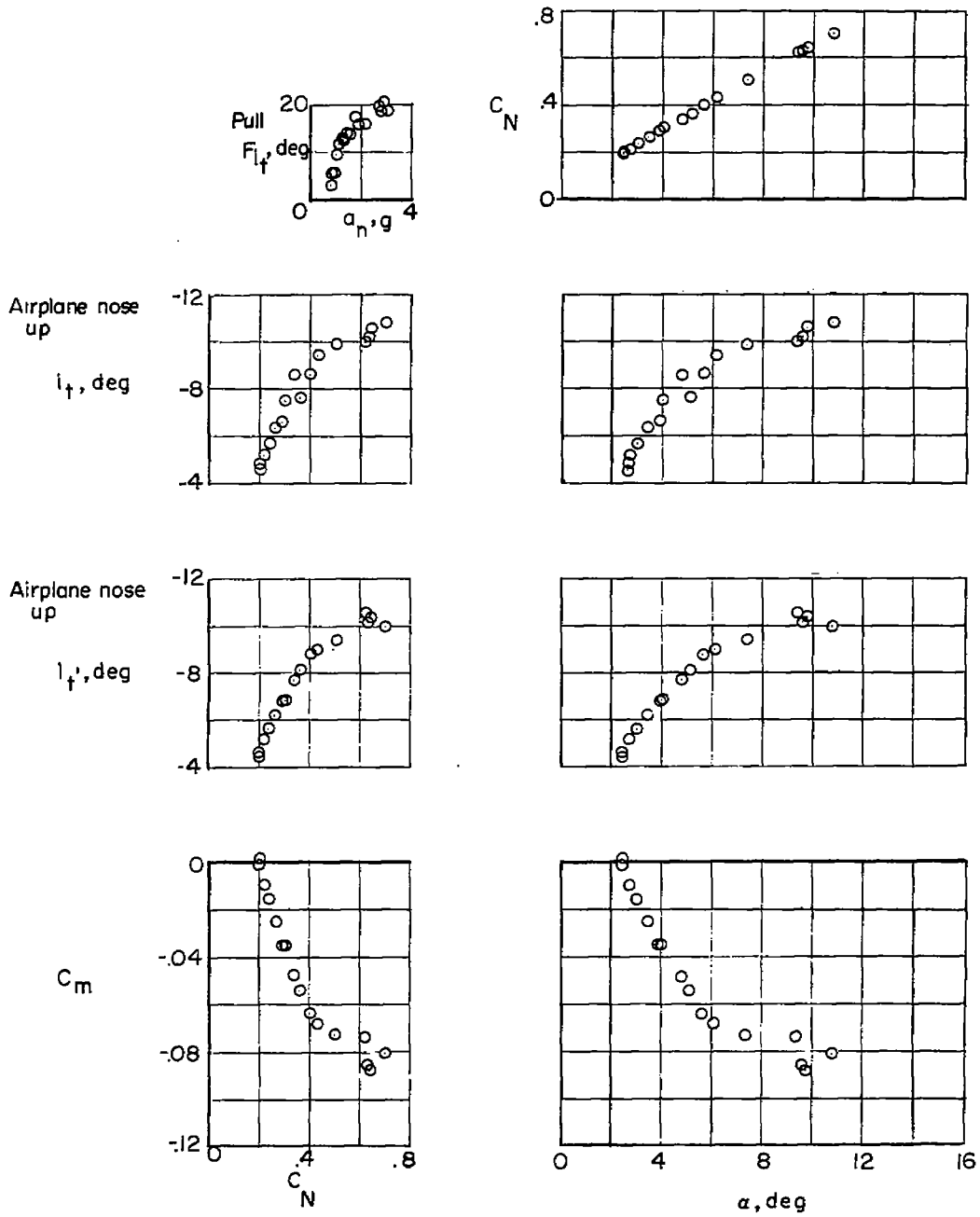
(c) $M \approx 1.135$; $h_p \approx 40,000$ ft.

Figure 9.- Concluded.



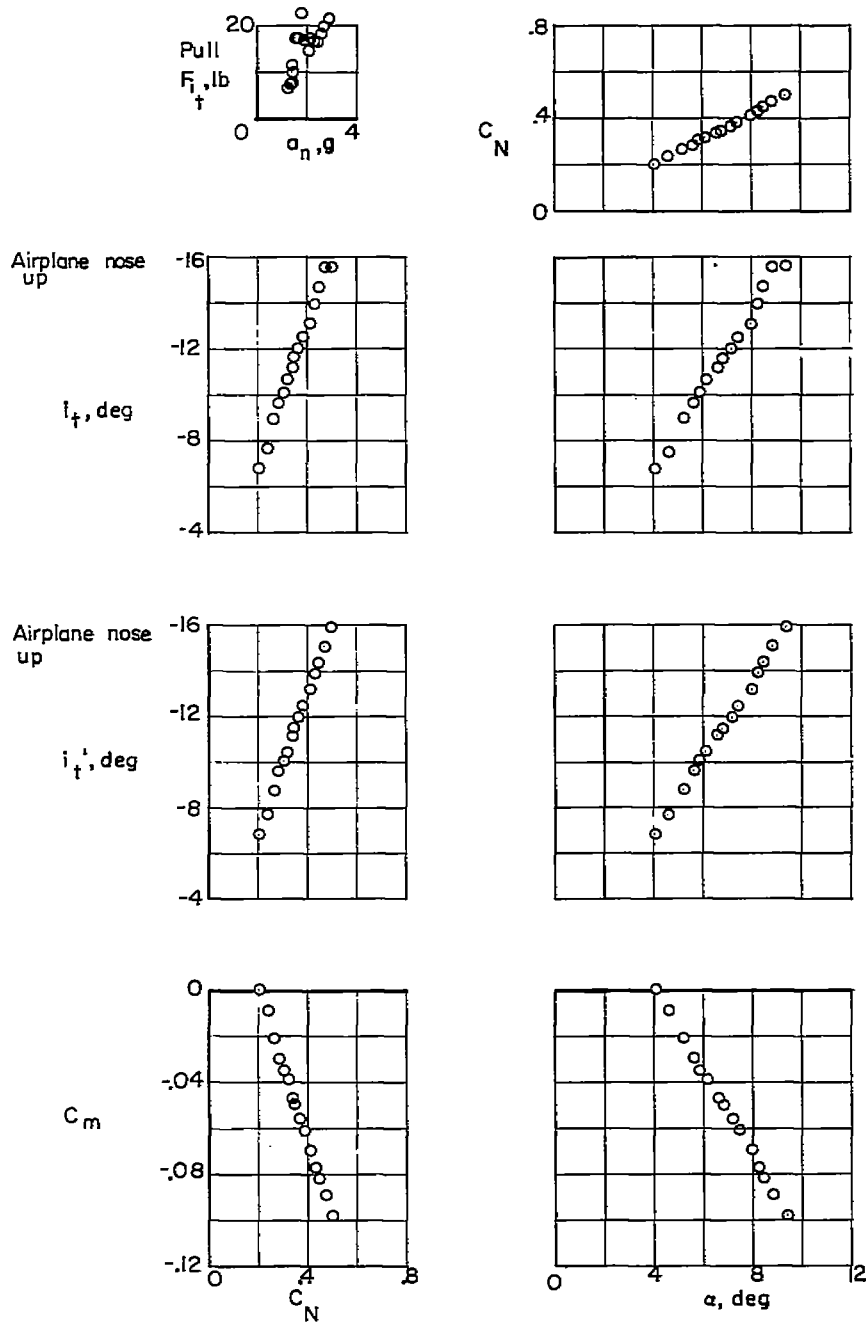
(a) $M \approx 0.880$; $h_p \approx 40,000$ ft.

Figure 10.- Variation of several stability and control characteristics during a wind-up turn. Two inboard slat segments locked closed.



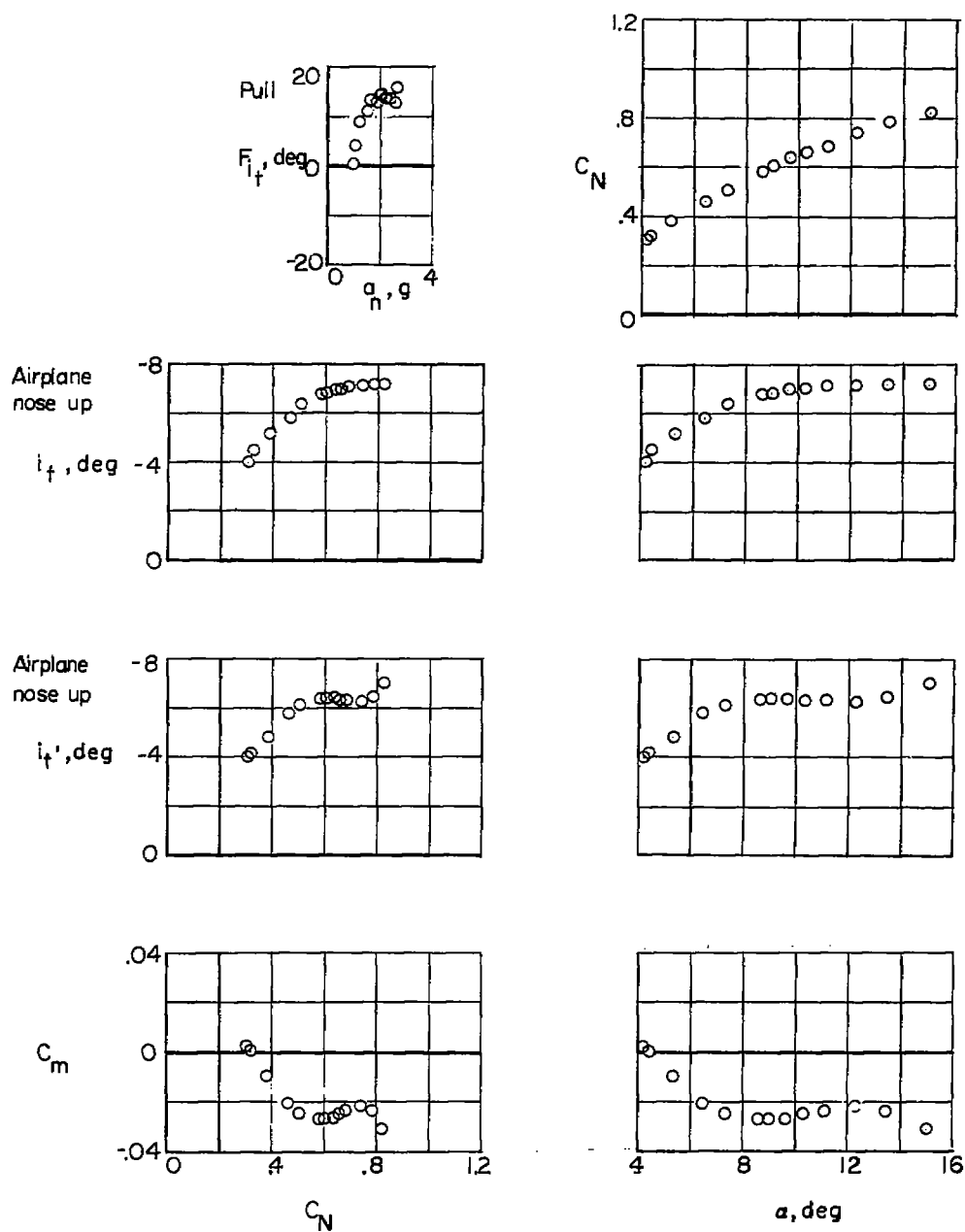
(b) $M \approx 0.955$; $h_p \approx 40,000$ ft.

Figure 10.- Continued.



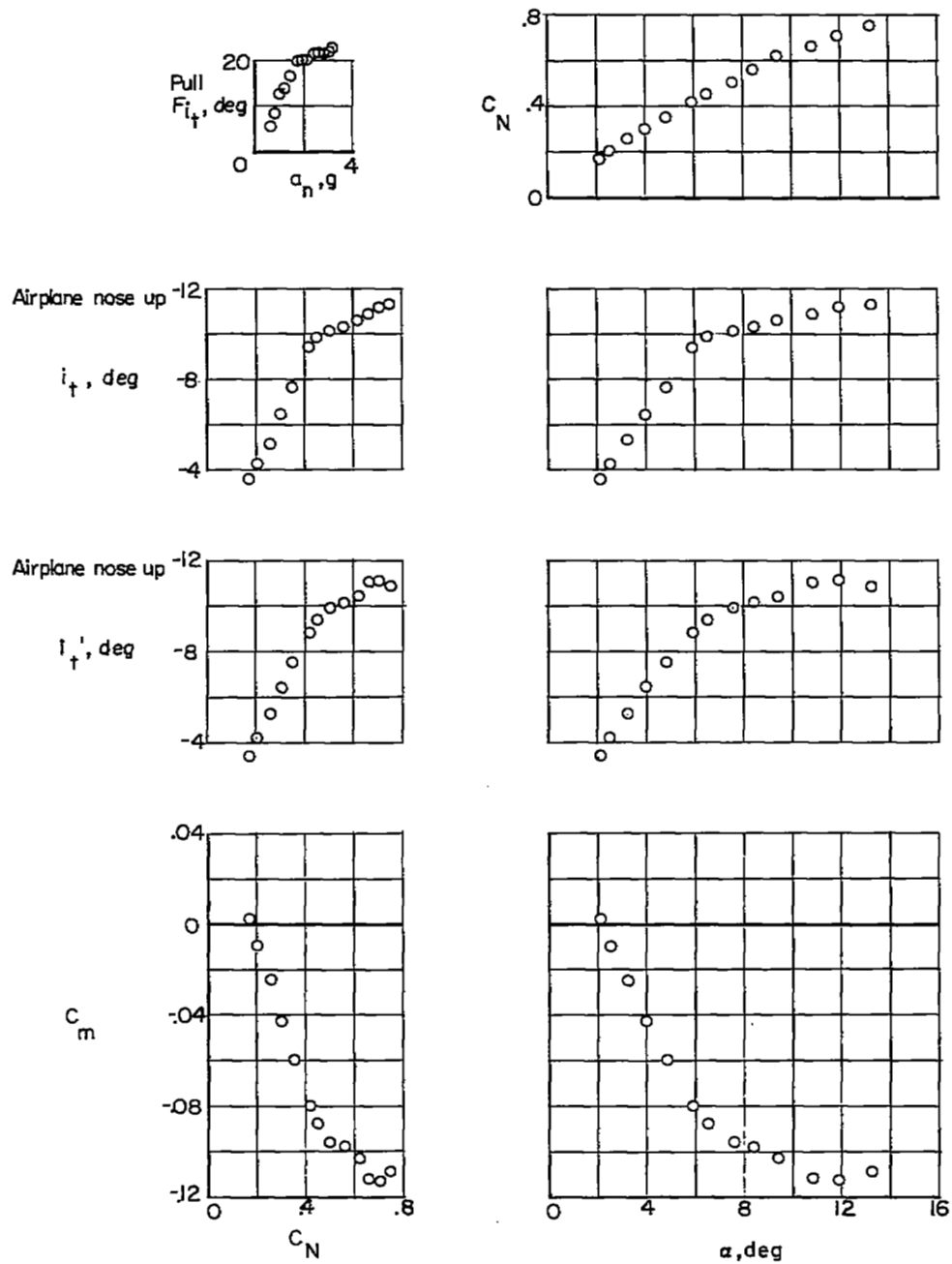
(c) $M \approx 1.150$; $h_p \approx 40,000$ ft.

Figure 10.- Concluded.



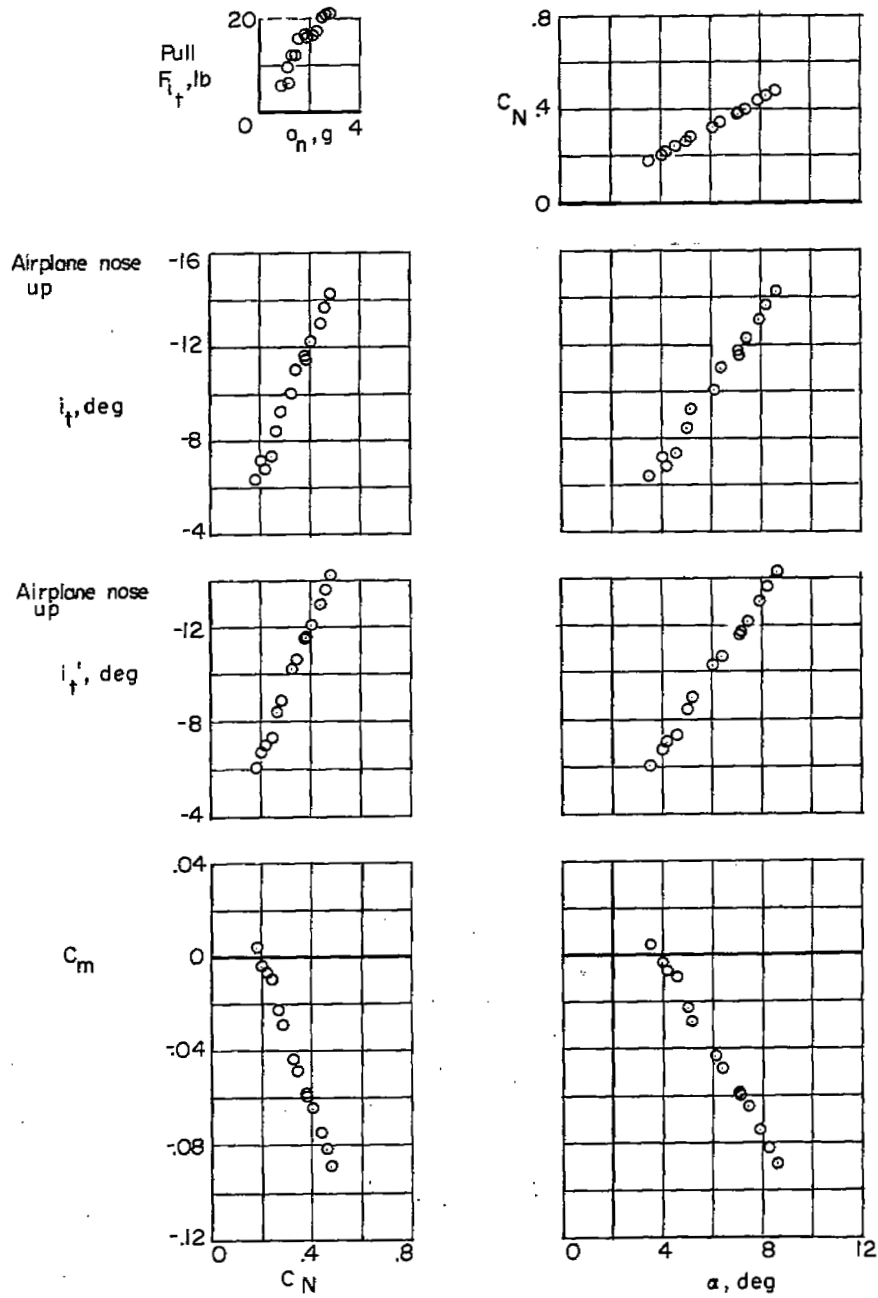
(a) $M \approx 0.875$; $h_p \approx 40,000$ ft.

Figure 11.- Variation of several stability and control characteristics during a wind-up turn. All slats locked closed.



(b) $M \approx 0.950$; $h_p \approx 40,000$ ft.

Figure 11.- Continued.



(c) $M \approx 1.115$; $h_p \approx 40,000$ ft.

Figure 11.- Concluded.

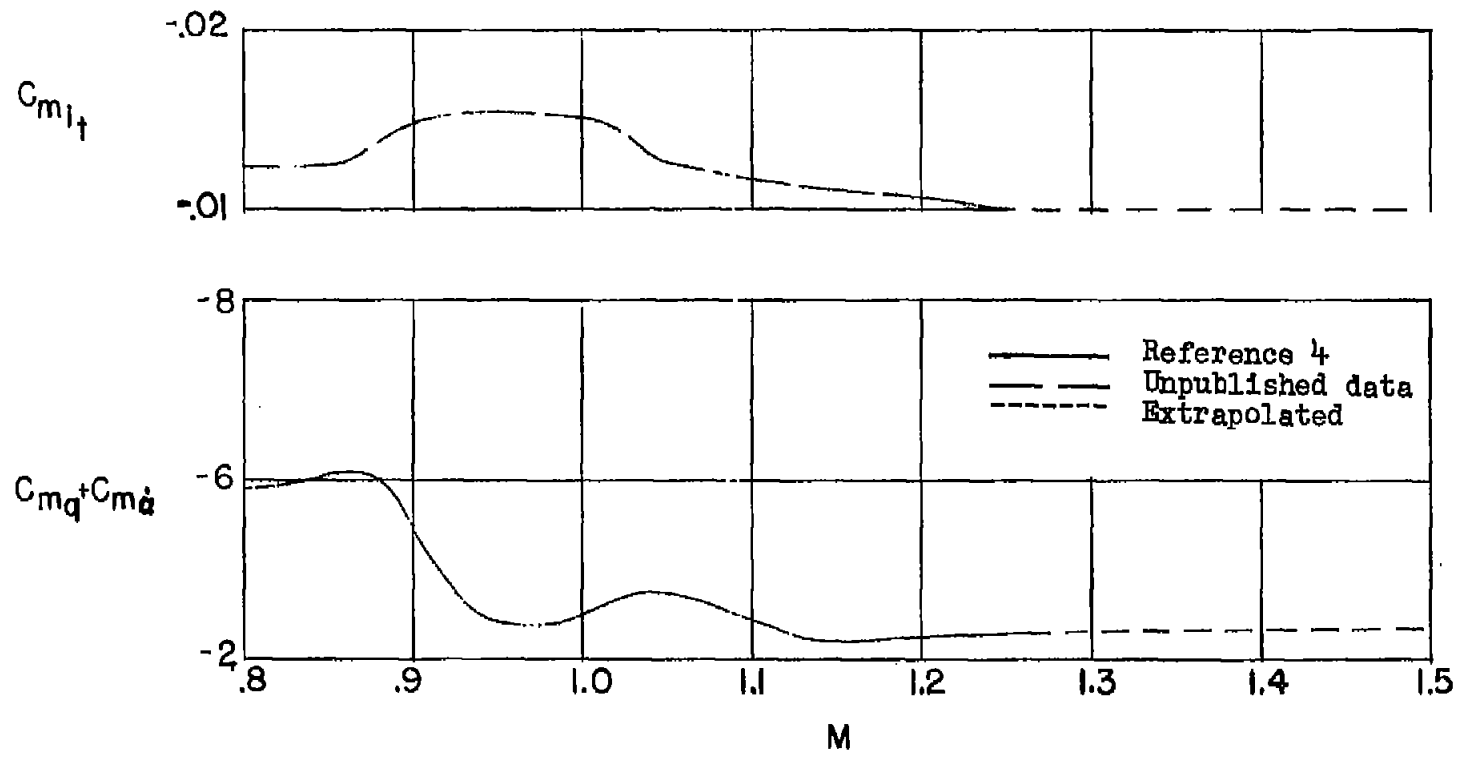


Figure 12.- Variation with Mach number of the stabilizer effectiveness and longitudinal damping parameters used to calculate pitching-moment curves.

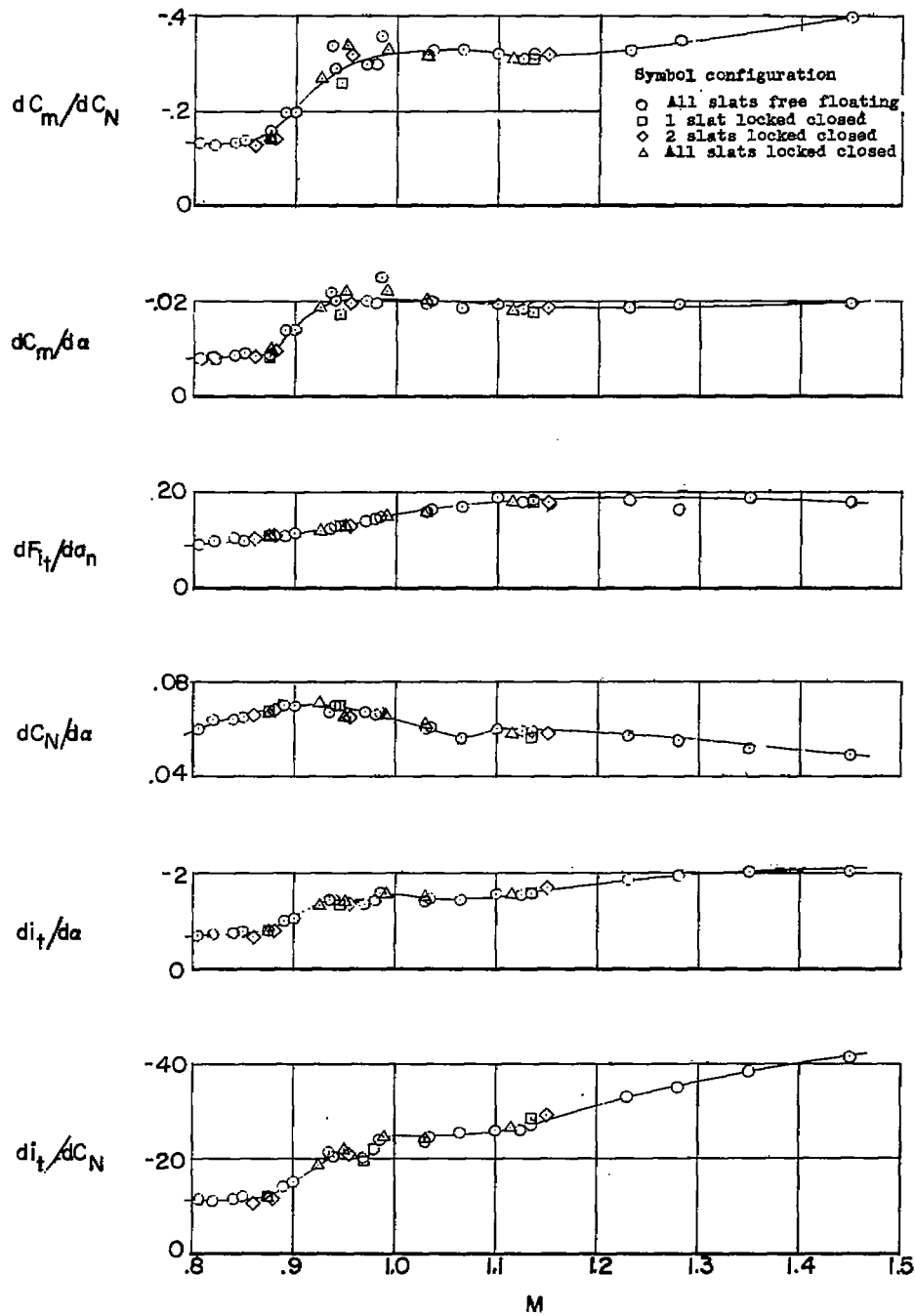
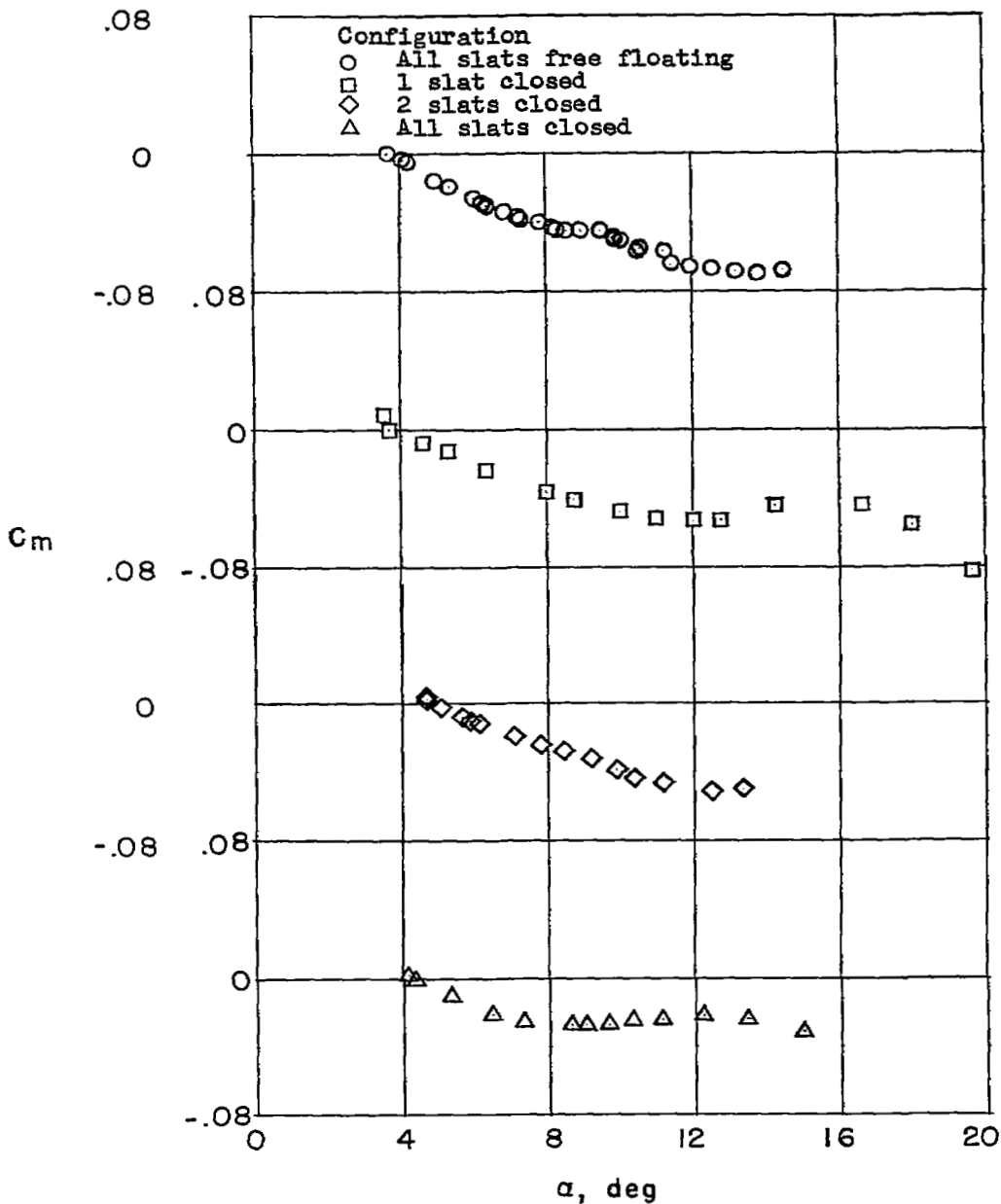
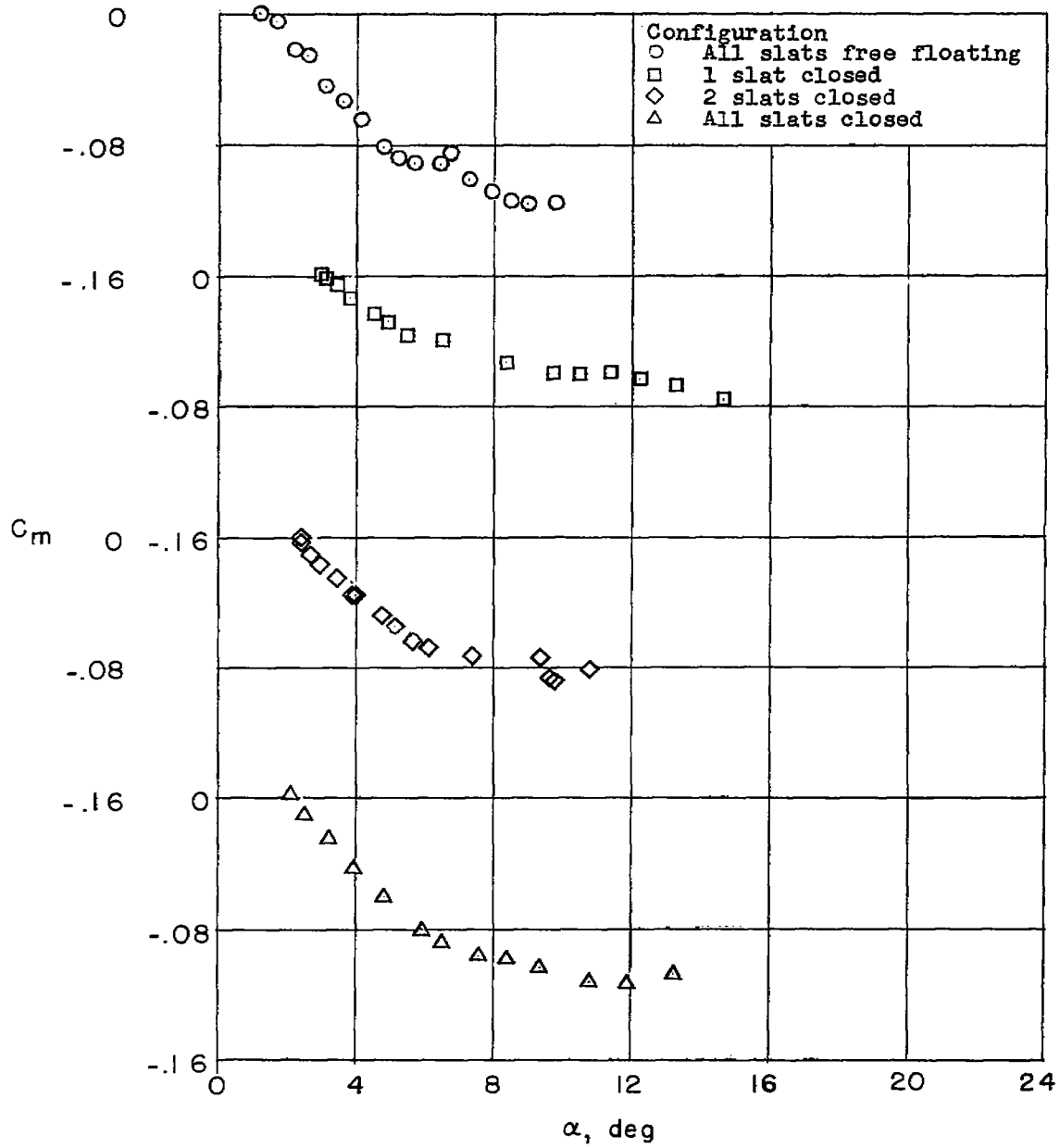


Figure 13.- Variation of longitudinal stability and control parameters with Mach number.



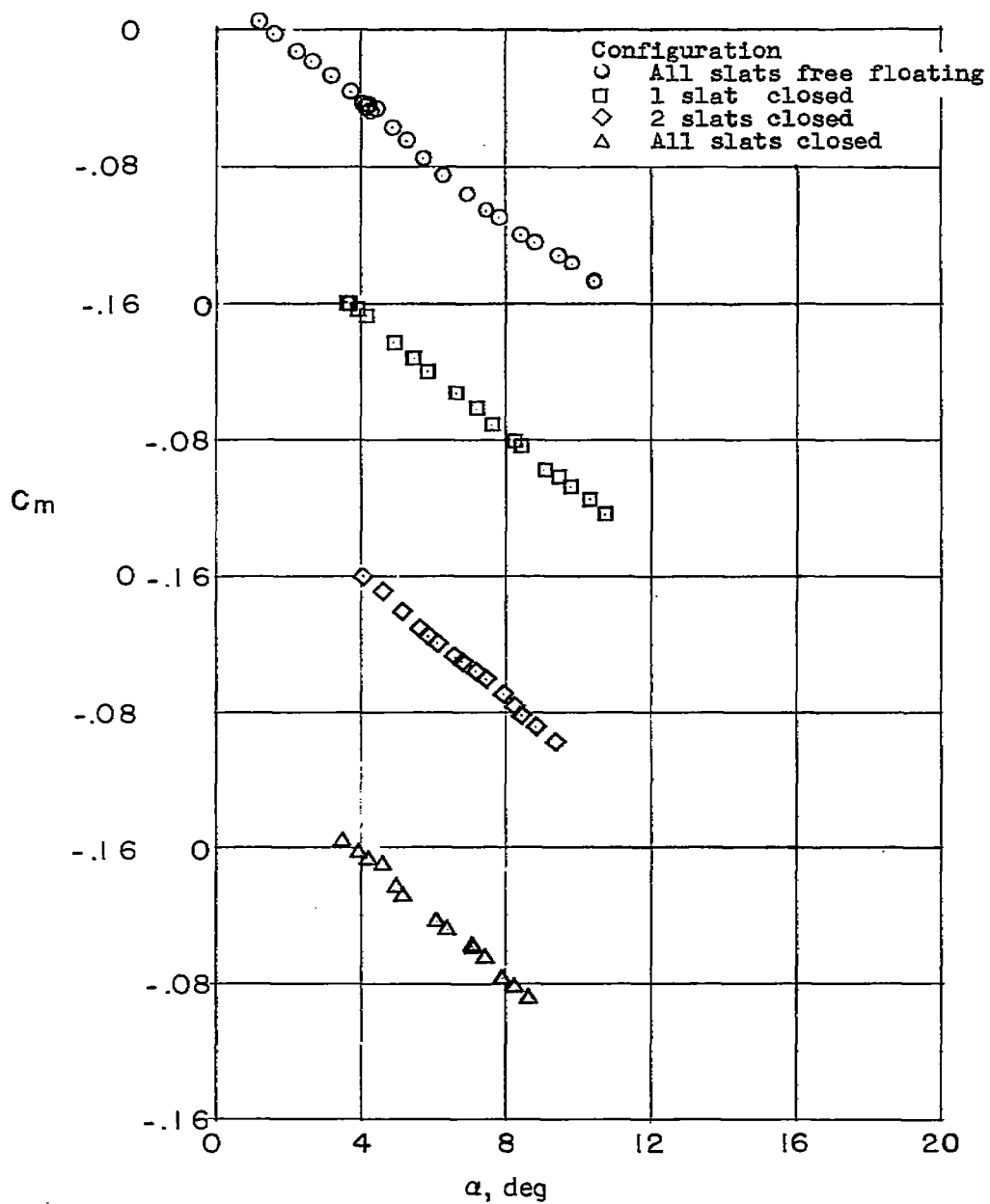
(a) M = 0.87.

Figure 14.- Comparison of pitching-moment-curve variation with angle of attack for the four configurations and three Mach numbers tested.



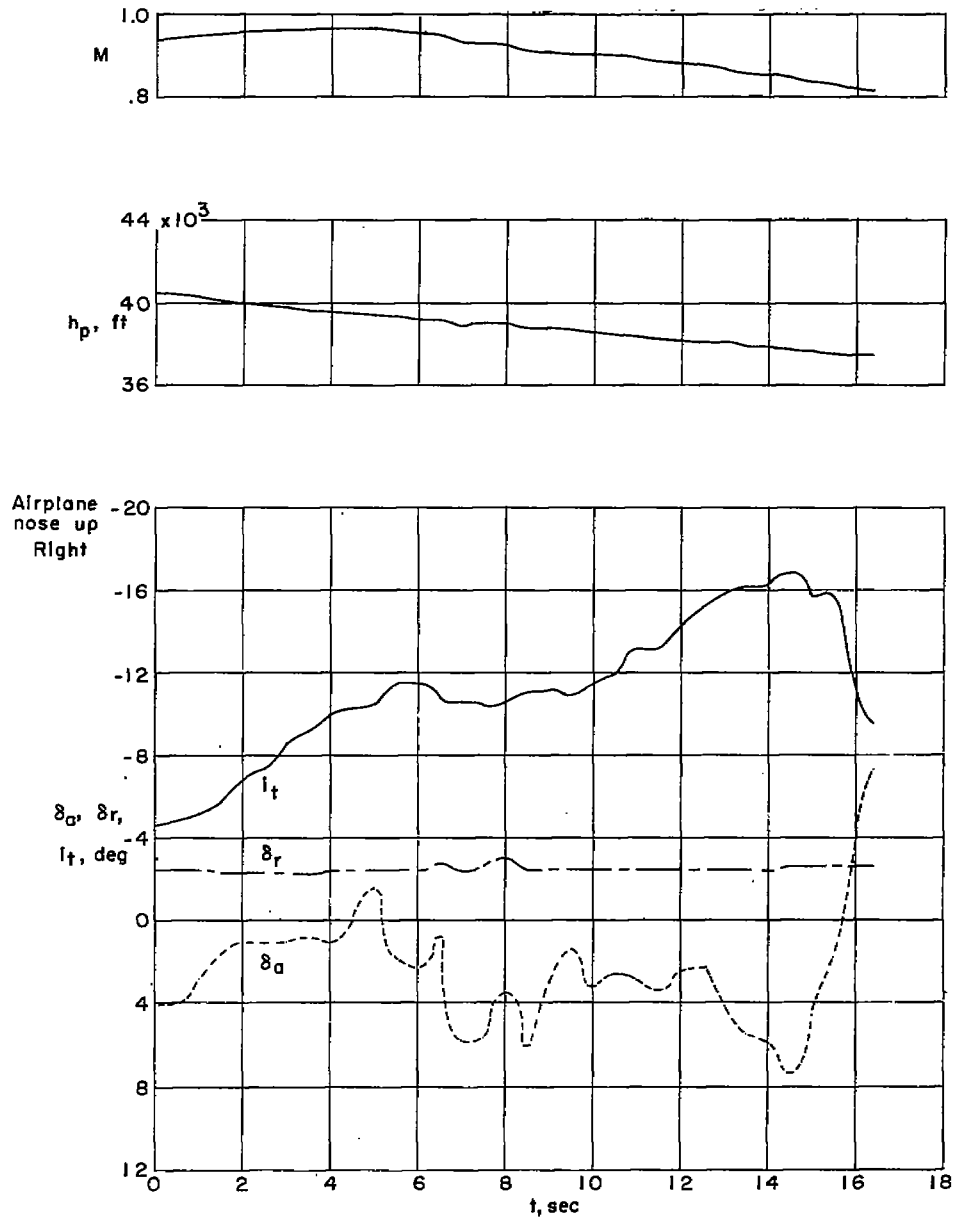
(b) $M = 0.95$.

Figure 14.- Continued.



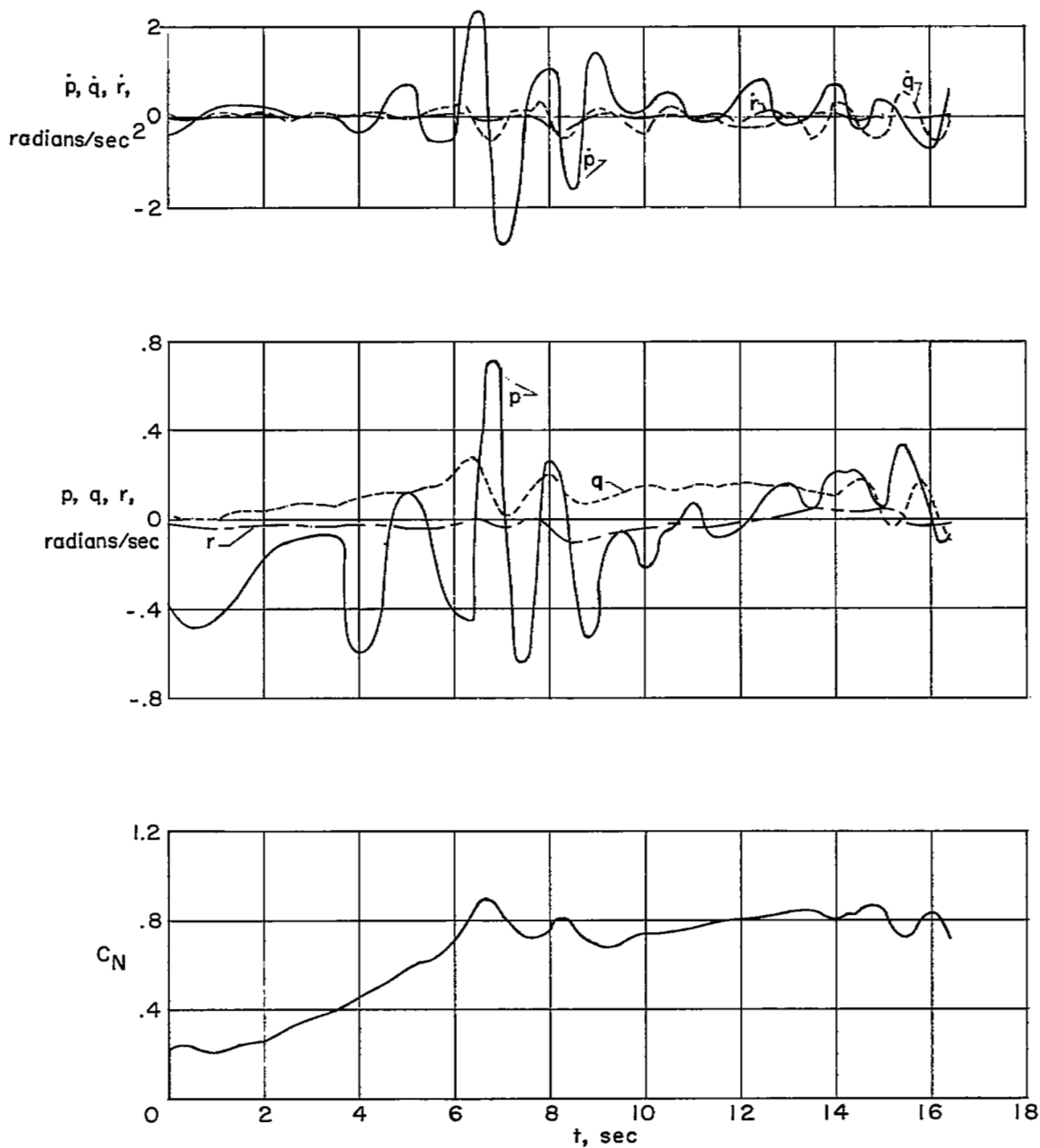
(c) $M = 1.13$.

Figure 14.- Concluded.



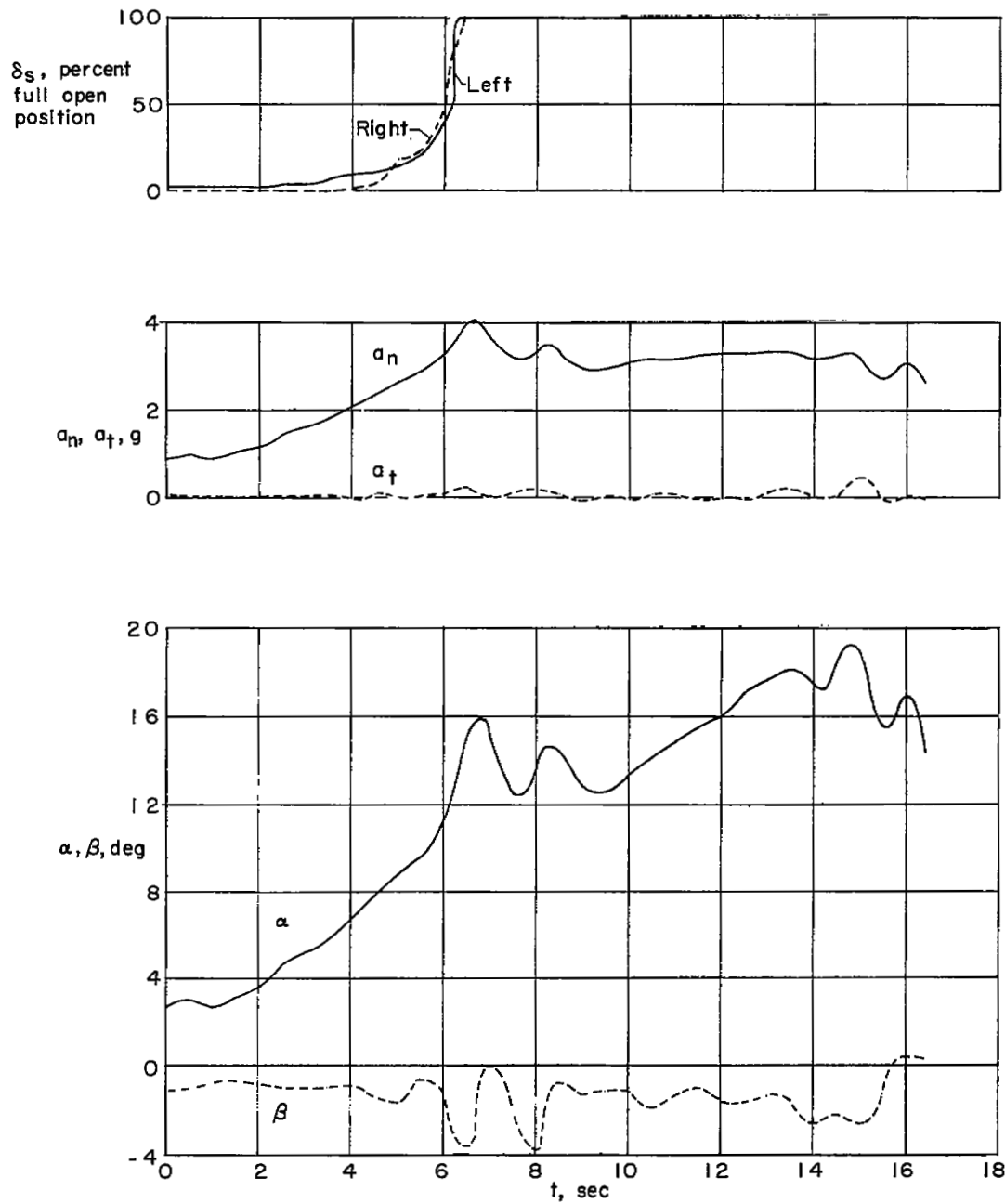
(a) Mach number, altitude, control deflections.

Figure 15.- Time history of a wind-up turn showing objectionable oscillatory motions, especially large rolling velocities and accelerations. Two slats locked closed; $M \approx 0.95$; $h_p \approx 40,000$ feet.



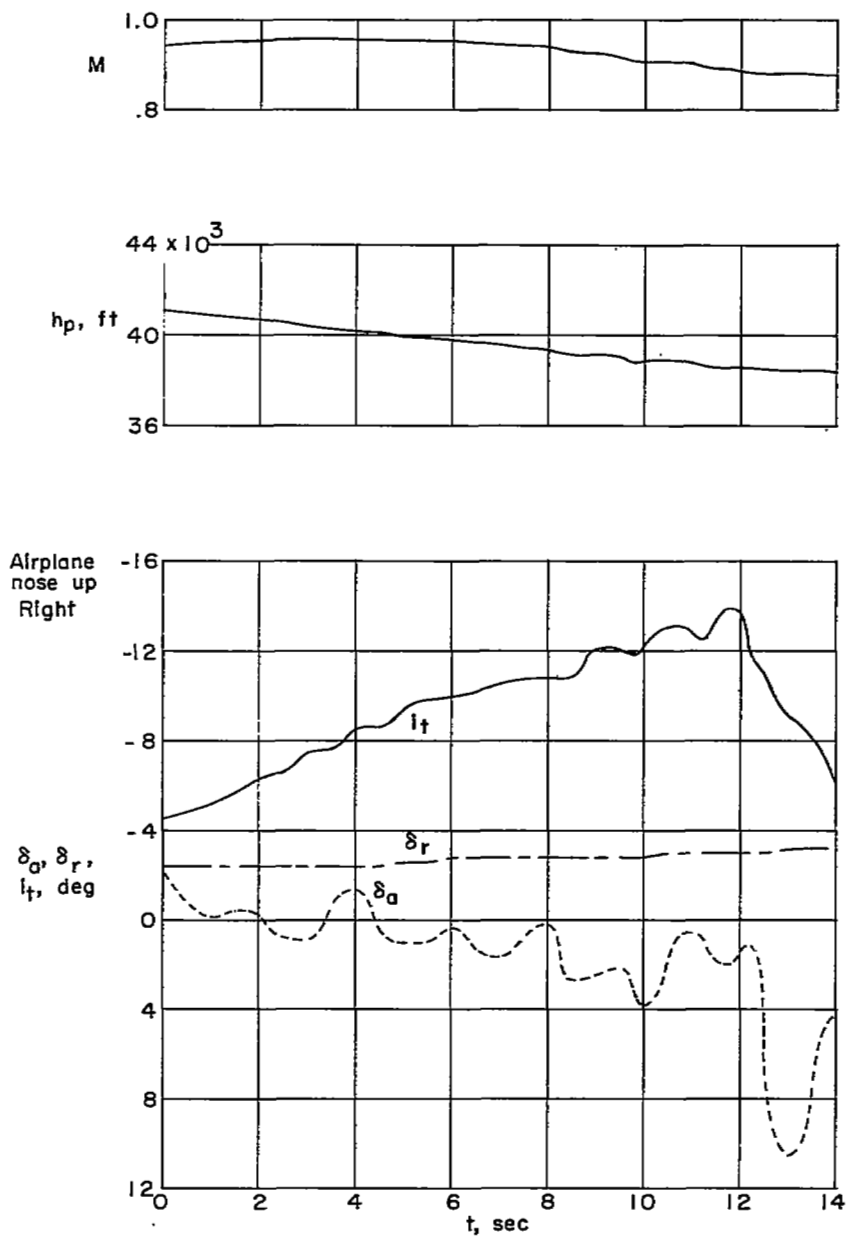
(b) Angular accelerations, angular velocities, and lift.

Figure 15.- Continued.



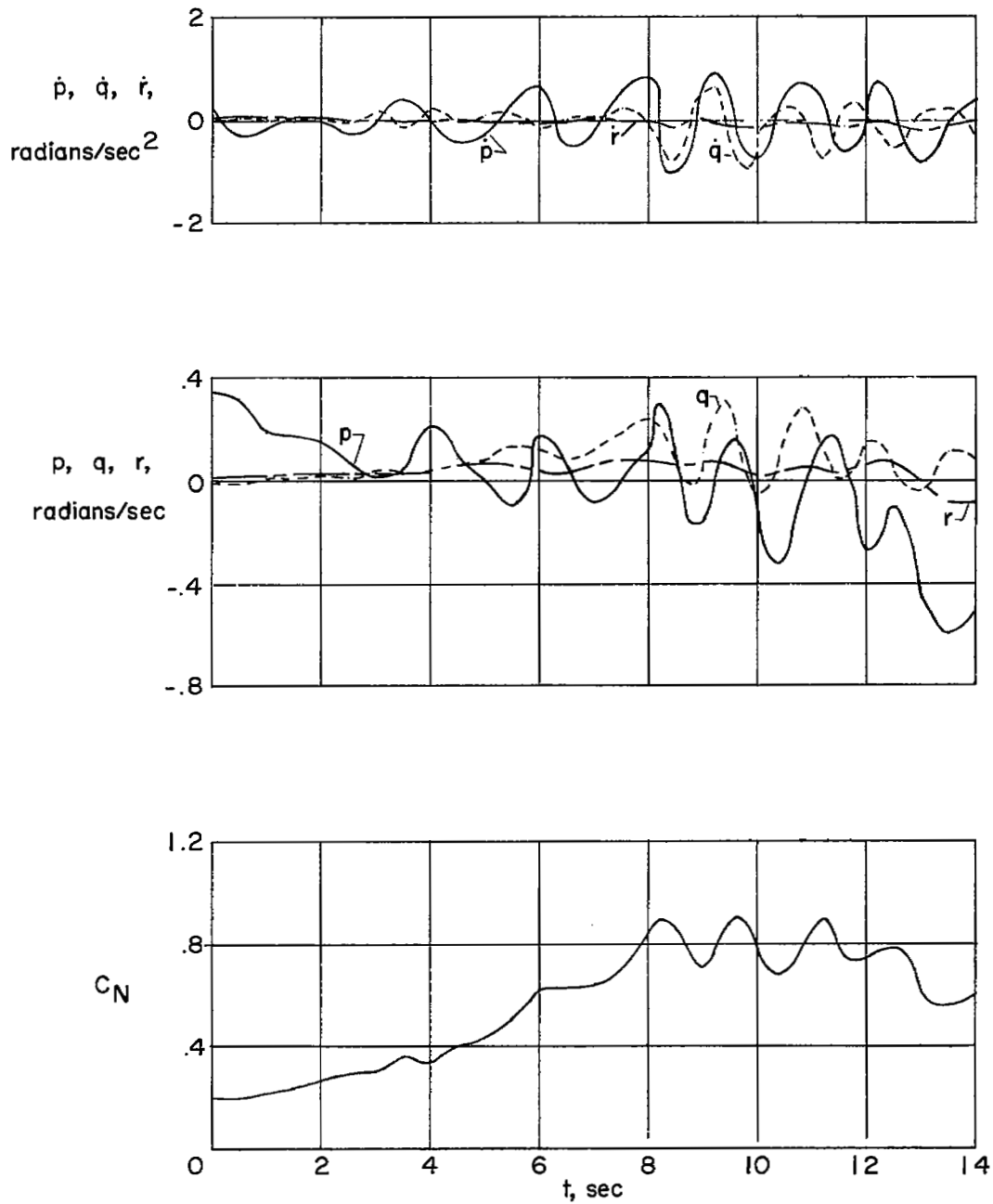
(c) Slat position, accelerations, angles of attack and sideslip.

Figure 15.- Concluded.



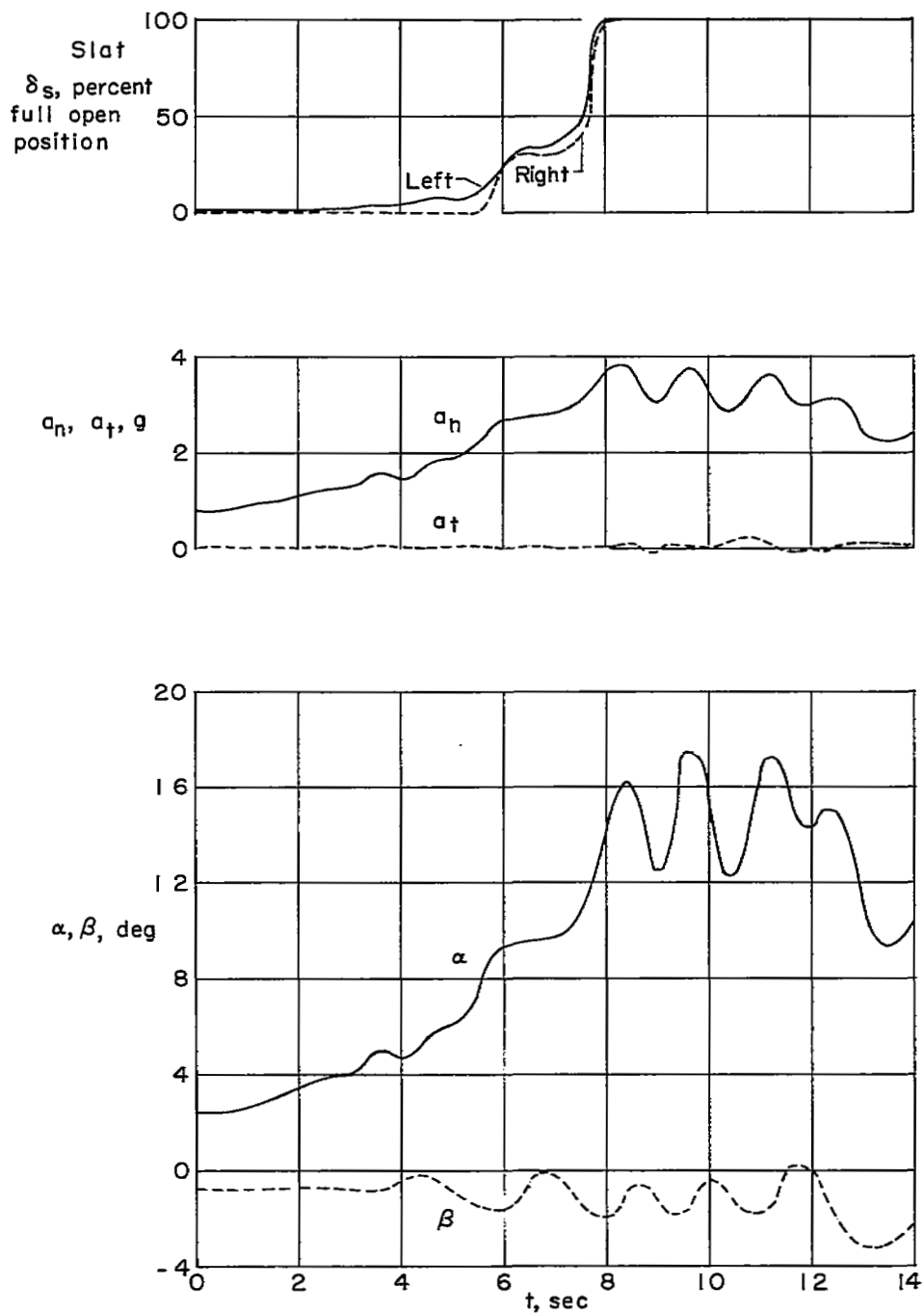
(a) Mach number, altitude, and control deflections.

Figure 16.- Time history of a wind-up turn showing objectionable oscillatory motions, especially large excursions in angle of attack. Two slats locked closed; $M \approx 0.95$; $h_p \approx 40,000$ feet.



(b) Angular accelerations, angular velocities, and lift.

Figure 16.- Continued.



(c) Slat position, accelerations, angles of attack and sideslip.

Figure 16.- Concluded.

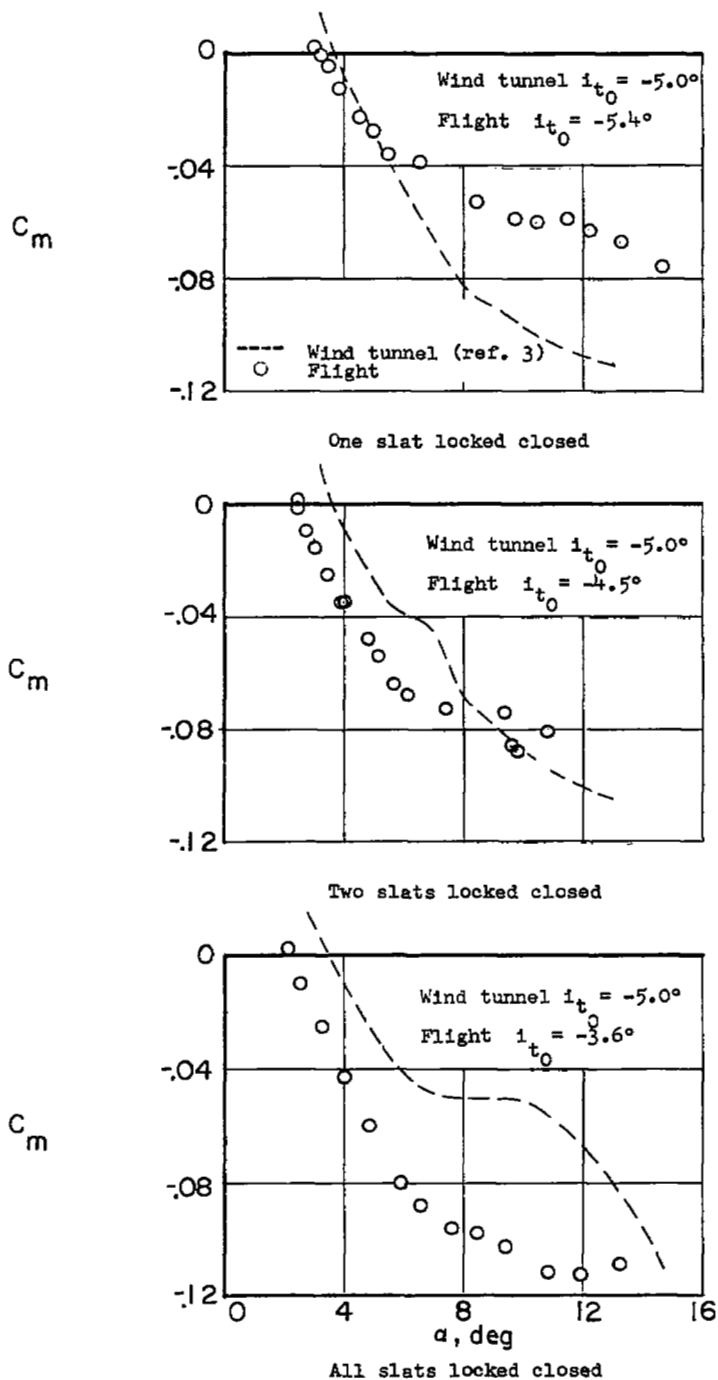


Figure 17.- Comparison of flight-test and wind-tunnel data at a Mach number of 0.95.



NASA Technical Library

3 1176 01437 0077

...

...

...

